T. J. Phesse,M. Buchert,E. Stuart,D. J. Flanagan,M. Faux,S. Afshar-Sterle,F. Walker,H.-H. Zhang,C. J. Nowell,R. Jorissen,C. W. Tan,Y. Hirokawa,M. F. Eissmann,A. R. Poh,J. Malaterre,H. B. Pearson,D. G. Kirsch,P. Provero,V. Poli,R. G. Ramsay,O. Sieber,A. W. Burgess,D. Huszar,E. Vincan,M. Ernst

Partial inhibition of gp130-Jak-Stat3 signaling prevents Wnt-beta-catenin-mediated intestinal tumor growth and regeneration
SCIENCE SIGNALING (2014) 7
DOI: 10.1126/scisignal.2005411

Instructions: Please use this document to start your revisions. Please enable track changes and do NOT delete the comments. Please respond to the comments by editing the comment balloon and adding your initials.

Editor summary:

A Novel Strategy for Treating Colon Cancer

In most patients, colon cancer arises from a mutation in the gene encoding APC, which results in constitutive activation of the β-catenin pathway. Inhibition of this pathway interferes with the continuous renewal of the epithelial cells that line the intestinal tract and therefore may confer only limited therapeutic benefit. Phesse *et al*. discovered that the signaling pathway involving the receptor gp130, the associated Jak kinases, and the transcription factor Stat3 enhanced the growth of intestinal tumors in mice. Conversely, genetic or pharmacological inhibition of this pathway reduced tumor growth by increasing the expression of genes encoding the p21 and p16 proteins that halt cell division, via a cell intrinsic mechanism. Thus, drugs targeting the Jak-Stat3 pathway, which are currently in clinical trials for the treatment of haematological malignancies, may also be useful for treating colon cancer.

Partial inhibition of gp130-Jak-Stat3 signaling prevents Wnt-mediated intestinal tumour growth and regeneration

Toby J. Phesse[1,#], Michael Buchert[1,#], Emma Stuart[1], Dustin J. Flanagan[2], Maree Faux[1], Shoukat Afshar-Sterle[1], Francesca Walker[1], Hui-Hua Zhang[1], Cameron J. Nowell[1], Robert Jorissen[1], Chin Wee Tan[1], Yumiko Hirokawa[1], Moritz Eissmann[1], Ashleigh R. Poh[1], Jordane Malaterre[3], Helen B. Pearson[3], David G. Kirsch[4], Paolo Provero[5], Valeria Poli[5], Robert G. Ramsay[3], Oliver Sieber[1], Antony Burgess[1], Dennis Huszar[6], Elizabeth Vincan[2] and Matthias Ernst[1,*]

[1] Ludwig Institute for Cancer Research, Melbourne, Australia *and* The Walter and Eliza Hall Institute of Medical Research, Melbourne, Australia *and* Department of Medical Biology, University of Melbourne, Australia

[2] Department of Anatomy and Cell Biology, University of Melbourne, VIC3052, *and* Victorian Infectious Diseases Reference Laboratories, North Melbourne, VIC3051 *and* School of Biomedical Sciences, Curtin University, Perth, WA6845, Australia.

[3] Peter MacCallum Cancer Centre, Melbourne, VIC3002, Australia *and* the Sir Peter MacCallum Department of Oncology, University of Melbourne, Parkville VIC3052, Australia.

[4] Departments of Radiation Oncology, Pharmacology and Cancer Biology, Duke University Medical Center, Durham, NC27710, USA.

[5] Department of Genetics, Biology and Biochemistry, University of Turin, 10126 Torino, Italy.

[6] AstraZeneca, Oncology iMed, Waltham, MA 02451, USA.

# Authors contributed equally

* Correspondence: matthias.ernst@wehi.edu.au

ABSTRACT

Most colon cancers arise from somatic mutations in the tumor suppressor gene *APC* and these mutations cause constitutive activation of the Wnt to β-catenin pathway in the intestinal epithelium. Because Wnt-β-catenin signaling is required for homeostasis and regeneration of the adult intestinal epithelium, therapeutic targeting of the Wnt pathway is challenging. We found that genetic activation of the cytokine-stimulated pathway mediated by the receptor gp130, the associated Jak kinases, and the transcription factor Stat3, was required for intestinal regeneration in response to irradiation-induced damage in wild-type mice and for tumorigenesis in *Apc*-mutant mice. Systemic pharmacological or partial genetic inhibition of gp130-Jak-Stat3 signaling suppressed intestinal regeneration, the growth of tumors in *Apc*-mutant mice, and the growth of colon cancer xenografts. Mechanistically, the growth of *Apc*-mutant tumors depended on gp130-Jak-Stat3 signaling for induction of the polycomb repressor Bmi-1, and the associated repression of genes encoding the cell cycle inhibitors p16 and p21. However, suppression of gp130-Jak-Stat3 signaling did not affect Wnt-β-catenin signaling or homeostasis in the intestine. Thus, these data not only suggest a molecular mechanism for how the gp130-Jak-Stat3 pathway can promote cancer, but also provide a rationale for therapeutic inhibition of Jak in colon cancer.

ONE SENTENCE SUMMARY

Partial suppression of the gp130-Jak-Stat pathway inhibits intestinal tumor growth.

INTRODUCTION

The lining of the mammalian intestine comprises a rapidly proliferating epithelial monolayer that undergoes continuous renewal (*1*). It provides two vital functions absorbing nutrients and water, and serving as a physical barrier that separates the immune system from luminal bacteria, antigens, and toxins. Tissue homeostasis of the adult intestinal epithelium depends on cellular plasticity to enable self-renewal, proliferation and apoptosis, and to ensure effective wound healing without promoting malignant outgrowth. These processes are regulated in part through Wnt-β-catenin signaling (*2, 3*), which promotes proliferation of the epithelial stem cell compartment at the base of the intestinal crypt and is required for intestinal regeneration (*4*). Wnt ligands are secreted glycoproteins that activate the Frizzled family of G-protein coupled receptors and the co-receptors Lrp5 and Lrp6. Activation of Wnt receptor complexes leads to inhibition of a protein complex, which includes the tumor suppressor protein APC (adenomatous polyposis coli) and prevents ubiquitin-mediated degradation of the transcriptional co-activator β-catenin (*5*). In greater than 80% of sporadic and familial colorectal cancers (CRC), mutations causing premature stop codons in *APC* induce constitutive accumulation and activation of β-catenin in the nucleus and drive tumor formation (*6, 7*).

Transcriptional regulation of many Wnt-β-catenin target genes, including the stem cell regulator Lgr5, is mediated through c-Myc (*7*). Systemic suppression of c-Myc in mice impairs homeostatic renewal of the intestinal epithelium (*8*), whereas ablation of *c-Myc* in intestinal epithelial cells (IECs) triggers repopulation from intestinal stem cells (*3*). Likewise, c-Myc is required for regeneration of intestinal crypts after γ-irradiation (*4*) and for intestinal hyperplasia in mice with conditional deletion of *Apc* in IECs (*7*). Therefore, therapies designed to interfere

with the Wnt-β-catenin pathway in CRC are likely to impact on homeostasis of the intestine, leading to dose-limiting toxicities and possibly limited clinical utility.

The gp130-Jak-Stat signaling pathway contributes to intestinal homeostasis, wound healing response and cancer (*9*). Binding to cytokines, including interleukin (IL) 6 or IL11, via their ligand specific receptor α-subunits causes homodimerization of the transmembrane receptor β-subunit gp130 and activation of Janus kinases (Jak1, Jak2, or Tyk2), which are constitutively associated with gp130. Jaks phosphorylate tyrosines in gp130 that then provide docking sites for the latent transcription factor Stat3, and also to some extent for Stat1. Subsequent tyrosine-phosphorylation of Stat3 by Jaks results in dimerization, nuclear translocation, and activation of Stat3-target genes, including *Socs3* and *Ccnd1* (*10*). IL11-dependent engagement of gp130-Jak-Stat3 pathway enables the intestine to respond to inflammatory stimuli that result from disruption of the protective epithelial monolayer (*11*). Accordingly, impairment of gp130-specific Stat3 activation in $gp130^{\Delta Stat/\Delta Stat}$ mice, in which the Stat3-binding region in gp130 is deleted, increases susceptibility to experimentally induced colitis (*12*). Conversely, activation of Stat3 confers resistance to colitis in $gp130^{F/F}$ mice, which contain a homozygous mutation that results in a Y757F amino acid substitution in gp130 that prevents binding of Socs3, a negative regulator of gp130-Jak-Stat3 signaling (*12*). Furthermore, excessive activation of Stat3 promotes colitis-associated colon cancer (*13*). Phosphorylation of Stat3 also occurs during the adenoma-to-carcinoma transition of in human colorectal cancer (*14*) and localizes to the invasive fronts of CRC tumors (*11*).

Here, we investigated the functional interaction between gp130-Jak-Stat and Wnt-β-catenin signaling pathways in CRC. We found that partial inhibition of the gp130-Jak-Stat3 pathway did not affect normal intestinal homeostasis but impaired regeneration of the intestinal epithelium in response to irradiation and slowed down the growth of tumors in *Apc*-mutant mice and mice with xenografts of human *APC*-mutant CRC cells. Manipulation of gp130-Jak-Stat3 signaling did not affect the expression of Wnt target genes in tumors, but increased the expression of the gene encoding the polycomb repressor Bmi-1. Similar to inhibition of gp130-Jak-Stat3 signaling, heterozygous knockout of *Bmi-1* in *Apc*-mutant mice reduced tumor growth and increased the abundance of the cell cycle inhibitors p16 (also known as Ink4a and encoded by *Cdkn2a*) and p21 (also known as Waf1 or Cip1 and encoded by *Cdkn1a*). Thus, the gp130-Jak-Stat3 pathway may serve as a "rheostat" to fine-tune the proliferative response of the intestinal epithelium during excessive activation of the Wnt-β-catenin pathway and therefore, may be amenable as a therapeutic target for *APC*-mutant CRC.

RESULTS

gp130-Jak-Stat3 signaling is required for intestinal regeneration in response to irradiation

We asked whether regeneration of the intestinal epithelium in response to radiation-induced damage required gp130-Jak-Stat3 signaling. We used immunohistochemistry for proliferating cell nuclear antigen (PCNA) to visualize proliferating IECs in regenerating intestinal crypts of mice 72 hours after 14Gy of whole body γ-irradiation (*4*). We examined mice with a heterozygous deletion that eliminates the Stat3-binding region of gp130 (*gp130*$^{\Delta Stat/+}$ mice) (*12*) or heterozygous deletion of *Stat3* (*Stat3*$^{+/-}$) (*15*). We found significantly fewer regenerating crypts in irradiated *gp130*$^{\Delta Stat/+}$ or *Stat3*$^{+/-}$ mice compared to irradiated wild-type mice (Fig. 1A). We also asked whether pharmacological inhibition of Jak-Stat signaling could affect regeneration buy using AZD1480, an ATP-competitive kinase inhibitor with specificity for Jak1 and Jak2 (*16*). We found that irradiated wild-type mice, which were gavaged daily with AZD1480 for the 3 days prior to irradiation and during the 72h follow-up period, displayed reduced epithelial regeneration compared to vehicle-treated, irradiated wild-type mice (Fig. 1A).

Wnt-β-catenin signaling is required for the regeneration of IECs after irradiation (*4*); thus, we examined whether Stat3 signaling was required for Wnt signaling in this context. Consistent with the presence of active Wnt-β-catenin signaling (*4*), we found that c-Myc and β-catenin accumulated in the nuclei of cells at the base of regenerating crypts in irradiated wild-type mice (Fig. 1B). We also detected nuclear c-Myc and β-catenin in cells of the stunted, nonregenerating crypts of irradiated *gp130*$^{\Delta Stat/+}$ mice (Fig. 1B). Likewise, expression of the β-catenin target genes *Lgr5, Fzd7*, *Axin2, Ccnd2, Cd44,* and *c-Myc* (*17*) was comparable between IECs of irradiated wild-type and *gp130*$^{\Delta Stat/+}$ mice (Fig. 1C). In contrast, irradiation-induced expression

of *Ccnd1*, which encodes the cell cycle regulatory protein cyclin D1 and is a target of both Wnt-β-catenin and gp130-Jak-Stat3 signaling, was reduced in irradiated $gp130^{\Delta Stat/+}$ mice compared to irradiated wild-type mice (Fig. 1C).

To assess whether Stat3 signaling was required in IECs for crypt formation, we analyzed the formation of organoids in three dimensional cell cultures established from isolated crypts of the small intestine and the colon (*18*). Organoids established from wild-type mice, and grown in media with the Stat3 inhibitor S3I-201 (*19*) or the Jak inhibitor AZD1480 had fewer crypt-like outgrowths than those grown in vehicle-containing medium (Figs. 1D and S1A and B**)**. In contrast, organoids established from $gp130^{F/F}$ mice, or those from wild-type mice grown in media containing IL11, had more crypt-like outgrowths than organoids established from wild-type mice and grown in control media (Figs. 1D and S1A and B**)**. Thus, gp130-dependent Stat3 signaling facilitates regeneration of IECs in parallel to Wnt-β-catenin signaling, and this is likely to occur by an IEC-autonomous mechanism.

gp130-Jak-Stat3 signaling is required for intestinal tumorigenesis caused by loss of Apc

Stat3 promotes colitis-associated colon cancer (*13*). We investigated whether gp130-Jak-Stat3 signaling was also required for intestinal tumorigenesis in the absence of overt colitis. We used mice heterozygous for the Apc^{Min} allele ($Apc^{Min/+}$ mice), which encodes a non-functional Apc protein similar to that found in human familial adenomatous polyposis. $Apc^{Min/+}$ mice undergo spontaneous somatic loss of the wild-type allele of *Apc* resulting in constitutive activation of β-catenin that leads to the formation of multiple tumors in the small intestine and colon (*20*). We found that genetic reduction of gp130-dependent Stat3 activation reduced the number and size of

tumors in the small and large intestines of $Apc^{Min/+}$; $gp130^{\Delta Stat/+}$ mice compared to $Apc^{Min/+}$ mice at 150 days of age (Fig. 2A). The few, small tumors that arose in $Apc^{Min/+}$; $gp130^{\Delta Stat/+}$ mice by 150 days of age were tubular adenomas (Fig. S1C) and did not progress to the invasive adenocarcinomas reported for mice with complete lack of Stat3 expression in IECs (*21*).

We also analyzed whether gp130-Jak-Stat3 signaling affected early stages of tumor formation by staining the colon of 100 day old $Apc^{Min/+}$ mice with methylene blue (*22*). $Apc^{Min/+}$; $Stat3^{+/-}$ mice had fewer methylene blue-positive foci than $Apc^{Min/+}$ mice (Fig. 2B and C). To assess whether activation of gp130-Jak-Stat3 signaling affected tumorigenesis in $Apc^{Min/+}$ mice, we used mice homozygous for the *gp130* mutation that results in the Y757F substitution in gp130 and prevents its negative regulation by Socs3 ($gp130^{F/F}$ mice) (*12*). We found that the colons of $Apc^{Min/+}$; $gp130^{F/F}$ mice had more and larger methylene blue-positive foci than $Apc^{Min/+}$ mice at 100 days of age (Fig. 2B and C). We confirmed that genetic manipulation of gp130-Jak-Stat3 signaling affected expression of the Stat3 target gene *Socs3* but the expression of the Wnt-β-catenin target gene *c-Myc* was comparable in intestinal tumors of $Apc^{Min/+}$; $gp130^{F/F}$, $Apc^{Min/+}$; $Stat3^{+/-}$, and $Apc^{Min/+}$ mice (Fig. S1D). We also assessed whether the increased tumor burden in $Apc^{Min/+}$; $gp130^{F/F}$ mice was a consequence of impaired MAPK signaling, which occurs in cells of $gp130^{F/F}$ mice as a consequence of the Y757F substitution mutation and prevents engagement of the Shp2-Erk signaling cascade (*12*). However, the phosphorylation of Thr202/Tyr204 of p42/44 MAPK was comparable in intestinal tumors of $Apc^{Min/+}$; $gp130^{F/F}$ and $Apc^{Min/+}$ mice (Fig. S1E). Thus, gp130-Jak-Stat signaling rather than gp130-dependent MAPK signaling was required for intestinal tumor initiation and growth in $Apc^{Min/+}$ mice.

gp130-Jak-Stat3 signaling affects tumor burden in *Apc*^{Min} mice independent of loss of *Apc* heterozygosity

Sustained activation of Stat3 can enable cells to overcome the DNA replication checkpoint response (*23*), leaving open the possibility that aberrant chromosome segregation in cells with altered gp130-Jak-Stat3 signaling could modify the kinetics of loss of heterozygosity of *Apc* in *Apc*$^{Min/+}$ mice. Therefore, we assessed the role of gp130-Jak-Stat3 signaling in tumorigenesis in mice with simultaneous inactivation of both alleles of *Apc* in intestinal stem cells. We expressed tamoxifen-inducible Cre-recombinase under the control of the intestinal stem cell marker *Lgr5* in mice with homozygous floxed alleles of *Apc* (*Lgr5*^{CreERT2}; *Apc*$^{fl/fl}$ mice) (*24*). We found that 35 days after tamoxifen injection, adult *Lgr5*^{CreERT2}; *Apc*$^{fl/fl}$ mice had tumors widespread throughout the small intestine and colon (Fig. 3A and fig. S2A). In contrast, tumours in both the small intestine and colon were significantly smaller when gp130-Jak-Stat3 signaling was reduced in *Lgr5*^{CreERT2}; *Apc*$^{fl/fl}$; *gp130*$^{\Delta Stat/+}$ mice (Fig. 3A and fig. S2A).

IEC-specific gp130-Jak-Stat3 signaling is required for the growth of *Apc* mutant intestinal tumors

In mice, immune cell-specific gp130-Jak-Stat3 signaling can enable anti-tumor immunity (*25*), while IEC-specific Stat3 facilitates colitis-associated colon cancer (*13*). To assess whether Stat3 was required cell autonomously in IECs for tumor growth, we selectively inhibited *Stat3* expression in IECs using *Lgr5*^{CreERT2} and a heterozygous floxed allele of *Stat3*. The small intestines and colons of *Lgr5*^{CreERT2}; *Apc*$^{fl/fl}$; *Stat3*$^{fl/+}$ mice were almost free of adenomas (Fig. 3A and S2A), and the few tumors that developed were tubular adenomas similar to those found in *Apc*$^{Min/+}$; *gp130*$^{\Delta Stat/+}$ mice (Fig. S1C). This is in stark contrast to the invasive behaviour of

tumors in *Apc*$^{Min/+}$ mice comprised of IECs with conditional homozygous deletion of *Stat3* (*21*). The latter had been attributed to compensatory increase in Stat1 abundance, which we also observed in tumors of *Lgr5*^{CreERT2}; *Apc*$^{fl/fl}$; *Stat3*$^{fl/fl}$ mice, when compared to tumors of *Lgr5*^{CreERT2}; *Apc*$^{fl/fl}$; *Stat3*$^{fl/+}$ or of *Lgr5*^{CreERT2}; *Apc*$^{fl/fl}$ mice (Fig. S4B). Collectively, this data suggests that partial inhibition of the gp130-Jak-Stat3 pathway impaired intestinal tumorigenesis through an epithelial cell intrinsic mechanism without changing the cellular behavior of the tumor cells.

Inhibition of gp130-Jak-Stat3 signaling does not affect the accumulation of β-catenin in *Apc*-mutant tumors

To explore the functional consequences of simultaneous activation of β-catenin and reduction of gp130-Jak-Stat3 signaling, we assessed the colocalization of nuclear β-catenin and PCNA (*24*) by immunohistochemistry. All tumors in *Lgr5*^{CreERT2}; *Apc*$^{fl/fl}$ mice, and the few small emerging tumors in *Lgr5*^{CreERT2};*Apc*$^{fl/fl}$; *gp130*$^{\Delta Stat/+}$ mice, labelled robustly for nuclear β-catenin (Fig. 3B) suggesting that high Wnt-β-catenin signaling persisted despite impaired gp130-Jak-Stat signaling. However, tumors in *Lgr5*^{CreERT2}; *Apc*$^{fl/fl}$; *gp130*$^{\Delta Stat/+}$ mice had significantly fewer cells that were positive for both nuclear β-catenin and PCNA than those from *Lgr5*^{CreERT2}; *Apc*$^{fl/fl}$ mice (Fig. 3B), indicating that high Wnt-β-catenin signaling was not sufficient to effectively promote cell proliferation in tumors with partially impaired gp130-Jak-Stat3 signaling.

Pharmacological inhibition of gp130-Jak-Stat3 signaling inhibits tumor initiation and growth

Various small molecules that target the catalytic activity of Jak are in clinical development as therapies for haematological malignancies (*26*). Therefore, we explored whether pharmacological inhibition of Jak kinases could replicate the benefit conferred by genetic reduction of gp130-Jak-Stat3 signaling. Oral daily gavage of AZD1480 reduced tumor burden in *Lgr5*^{CreERT2}; *Apc*$^{fl/fl}$ mice when assessed 35 days after administration of tamoxifen (Figs. 4A and S2A). Furthermore, in *Apc*$^{Min/+}$ mice, administration of AZD1480 from 6 to 12 weeks of age reduced the number of tumors and decreased tumor size compared to those from mice treated with vehicle alone (Fig. 4B), suggesting that Jak inhibition prevented the formation of new tumors and blocked the growth of existing ones. These data suggest that pharmacological inhibition of Jak may be relevant for the treatment of human CRC.

Inhibition of the gp130-Jak-Stat3 pathway causes growth arrest in human CRC cells with mutation in the Apc-β-catenin pathway

We asked if co-activation of Stat3 and β-catenin occurs in human CRC and is required for the growth of established human CRC tumors. We evaluated gene expression in two independent cDNA microarray data sets from CRC patients (*27, 28*). We observed a marked increase of target genes for the Wnt-β-catenin (*17, 29*) and Stat3 signaling pathways (*30, 31*) in human CRC samples when compared to matched normal colons (Fig. S3).

In order to assess whether inhibition of Jak activity conferred therapeutic benefits to advanced-stage human CRC xenografts in mice, we administered AZD1480 to immune-compromised mice (BALB/c-nude) carrying CRC cell line xenografts of SW480 (mutant for *APC*, *KRAS*, *TP53*), DLD1 (mutant for *APC*, *TP53*, *PIK3CA*), LIM1899 (mutant for *CTNNB1* encoding β-catenin,

KRAS), or RKO (mutant for *PIK3CA*, *BRAF*) cells. AZD1480 inhibited the growth of xenografts from all cell lines with mutations in the Apc-β-catenin pathway, but not from RKO cells (Fig. 5A and S4A). Complete ablation of Stat3 in mouse embryo fibroblasts can induce a compensatory increase in Stat1, thereby skewing the IL6 response towards a Stat1-interferon-γ-dependent pathway and associated anti-tumour immune response (*32*). However, the abundance of Stat1 (Fig S4B) and the expression of the prototypic interferon-γ-Stat1 pathway target gene *IP-10* (*32*) were unaffected in SW480 xenografts of AZD1480-treated mice when compared to vehicle-treated mice (Fig. S4C). Since the BALB/c-nude host mice are also immune compromised, these results collectively support the notion that inhibition of gp130-Jak-Stat3 signaling limits tumor growth through mechanisms independent of restoring the adaptive anti-tumor immune response (*25*).

The observation that AZD1480 did not inhibit the growth of RKO xenografts suggested that the gp130-Jak-Stat3 pathway may be rate limiting only in CRC cells with mutations that confer constitutive activation of β-catenin. To directly test this hypothesis, we used an isogenic pair of CRC cell lines comprising parental SW480 cells, which express only mutated *APC*, and SW480^{APC} cells, which are engineered to re-express wild-type *APC* (*33*). Compared to parental SW480 cells, SW480^{APC} cells had reduced abundance of total and nuclear β-catenin and consequently reduced ability to activate a Wnt reporter (TOPFLASH) (Fig. S5A and B). When exposed to IL11, a gp130-activating cytokine that plays a major role in the gastrointestinal epithelium (*11*), SW480 and SW480^{APC} cells showed a similar increase in Tyr^{705} phosphorylated Stat3, which was abrogated by simultaneous exposure to AZD1480 (Figs. S5C and D). However, exposing SW480 or SW480^{APC} cells to AZD1480 or IL11 did not alter the abundance or

localization of β-catenin or the activity of TOPFLASH (Fig. S5A, C and E). Meanwhile addition of AZD1480 or S3I-201 impaired colony formation in soft agar of SW480, but not of SW480^{APC} cells (Figs. 5B), despite reducing the expression of *SOCS3* in both cell lines (Fig. S5F). Exposure to IL11 increased colony formation of both SW480 and SW480^{APC} cells (Fig. 5B), suggesting that gp130-Jak-Stat3 signaling can stimulate IEC proliferation irrespective of *APC* mutational status. Exposing SW480 or SW480^{APC} cells to an inhibitor of the epidermal growth factor receptor, which is frequently overexpressed in CRC (*34*) and may mediate Stat3 activation during epithelial regeneration of the midgut in flies (*35*), did not affect colony formation (Fig. 5B) or SOCS3 expression (Fig. S5F). Thus, Jak-mediated activation of Stat3 was rate-limiting for the proliferative response of SW480 cells with constitutive activation of β-catenin, suggesting a specific role of gp130-Jak-Stat3 signaling in tumor cells with aberrant β-catenin signaling.

Inhibition of gp130-Jak-Stat3 signaling does not affect intestinal homeostasis

We observed that gp130-Jak-Stat3 signaling regulated intestinal regeneration without altering expression of Wnt-β-catenin target genes (Fig. 1B and C). To investigate whether inhibition of gp130-Jak-Stat signaling impaired tumor formation also without affecting the high aberrant Wnt-β-catenin signaling observed in *Apc*-mutant CRC xenografts, we monitored gene expression. As expected, we observed that SW480 tumors from AZD1480-treated mice had reduced expression of the STAT3 target genes *SOCS3* and *CCND1*, but not of the Wnt-β-catenin target genes *MYC* and *LGR5* compared to vehicle-treated mice (Fig. 6A). Likewise, immunohistochemical analysis revealed similar amounts of β-catenin and the protein encoded by the Wnt-β-catenin target gene *CD44* in SW480 xenografts from AZD1480-treated and vehicle-treated mice (Fig. S7B).

Stat3 is essential for survival of intestinal stem cells (*36*), and therefore, inhibition of gp130-Jak-Stat3 signaling could affect normal intestinal homeostasis. We analysed non-cancerous regions of the small intestines and colons of BALB/c-nude mice carrying SW480 xenografts, which were injected with 5-bromo-2'-deoxyuridine (BrdU) and gavaged daily with AZD1480 or vehicle control for 14 days. In addition, we labelled sections of these intestines with the periodic acid-Schiff (PAS) method to detect mucins (*37*) and with antibodies to detect lysozyme, a marker of Paneth cells (*38*). This analysis revealed a comparable size of the proliferative and differentiated IEC compartments in the small intestines of AZD1480- and vehicle-treated mice (Fig. S6A). Moreover, the positioning of Paneth cells, which is disrupted by excessive Wnt-β-catenin signaling (*17*), was similar in AZD1480- and vehicle-treated mice (Fig. S6A). Consistent with this observation, the expression of Wnt-β-catenin target genes was similar in IECs isolated from AZD1480- and vehicle-treated mice (Fig. S6B). Disruption of intestinal homeostasis can lead to loss of body weight; however, up to two weeks of AZD1480 administration did not affect total body weight in these mice (Fig. S6C). Thus, partial systemic inhibition of gp130-Jak-Stat3 signaling had no overt effects on intestinal homeostasis, and is likely to be well tolerated.

gp130-Jak-Stat3 signaling suppresses cell cycle inhibition by p16 and p21 upregulation via the corepressor Bmi-1

We hypothesized that inhibition gp130-Jak-Stat3 activation may induce growth arrest in *Apc*-mutant cells. Intestinal tumors of *Lgr5*^{CreERT2}; *Apc*$^{fl/fl}$; *gp130*$^{\Delta Stat/+}$ mice had increased abundance of the cell cycle inhibitor p21 compared to tumors in *Lgr5*^{CreERT2}; *Apc*$^{fl/fl}$ mice (Fig. S7A). Likewise, tumors in *Apc*$^{Min/+}$; *gp130*$^{\Delta Stat/+}$ mice had increased abundance of p16 (Fig. 6B) and p21 (Fig. 6C) compared to tumors in *Apc*$^{Min/+}$ littermates. Similarly, SW480 xenografts from

AZD1480-treated mice had increased abundance of p21 (Fig. 6D) and expression of *CDKN1A*, the mRNA encoding p21 (Fig. 6A) than tumors in vehicle-treated mice.

Because the polycomb-group protein Bmi-1 transcriptionally represses *Cdkn1a and Cdkn2a*, which encodes p16 (*39*), we investigated whether gp130-Jak-Stat3 signaling affects the amount of Bmi-1. Expression of *Bmi1* was increased in IECs isolated from $gp130^{F/F}$ mice compared to those from wild-type mice (Fig. S7C). Injection of IL11 also increased the expression of *Socs3* and *Bmi1* in IECs isolated from $gp130^{F/F}$ mice (Fig. S7D). In contrast, the Bmi-1 mRNA (Fig. 6A) and protein (Fig. S7B) were reduced in SW480 xenografts from AZD1480-treated mice compared to vehicle-treated mice.

We analyzed whether Bmi-1 was a direct target of Stat3. Sequence analysis of *Bmi1* identified a putative Stat3-binding site in intron 1 starting at nucleotide position 4077 (Fig. S7E), and which was similar to the Stat3 consensus binding motif CTCNNNGAG (*40*). Moreover, exposing SW480 cells to IL11 increased chromatin immunoprecipitation (ChIP) of a region of intron 1 of *BMI1* using an antibody for Stat3 (Fig. 6E). We created a luciferase reporter construct containing a region (base pairs 18681328-18681883; chr 2 of intron 1 of *Bmi1*. Exposing human embryonic kidney (HEK)293T cells to Hyper-IL6, a designer fusion protein comprising IL6 and the soluble part of the IL6Rα (*41*) significantly increased the activity of this reporter (Fig. S7F) to a similar degree as other reporters with single intronic Stat3-binding sites (*42*). Thus, these data support the conclusion that Stat3 directly binds to *Bmi1* and induces its transcription in a gp130-Jak-Stat3 signaling-dependent manner.

We directly tested whether *Bmi1*was required for intestinal tumor growth in mice. Heterozygous knockout of Bmi-1 ($Bmi1^{+/-}$) decreased the size of tumors (Fig. 6F) and increased the abundance of p21 and p16 in tumors (Figs. 6B and C) in the small intestine when crossed on to a $Apc^{Min/+}$ mutant background. Collectively, these data suggest that gp130-Jak-Stat3 signaling is rate-limiting for the growth of *Apc*-mutant intestinal tumors by repressing expression of the cell cycle inhibitors p21 and p16 through induction of the transcription of *Bmi1* (Figure summary).

DISCUSSION

Wnt-β-catenin signaling is required for the homeostasis and regeneration of the intestinal epithelium (*4, 5*) and is an etiological factor for the progression of intestinal tumors (*43*). Here, we found that inhibition of the gp130-Jak-Stat3 pathway limits the proliferative response of IECs during intestinal regeneration and tumorigenesis.

Excess activation of Stat3 in IECs due to the release of inflammatory cytokines by infiltrating myeloid cells suppresses apoptosis and promotes proliferation in mouse models of colitis-associated CRC (*13*). Here, we found that genetic activation of the gp130-Jak-Stat3 pathway promotes the formation of intestinal tumors in the absence of overt inflammation and is required for regeneration of intestinal epithelia in response to γ-irradiation. Systemic reduction of *Stat3* expression or suppression of gp130-mediated activation of Stat3 reduced the number and size of tumors and impaired regeneration in the intestine. Likewise, IEC-specific reduction of Stat3 expression also reduced tumorigenesis that resulted from *Apc* gene inactivation. Furthermore, the growth of xenografts of human *APC*-mutant CRC cell lines in immune-compromised mice was impaired by systemic administration of AZD1480. Human CRC cells, irrespective of their *APC* status, had basal STAT3 activity, which was modulated in response to inhibition or IL11-mediated stimulation of gp130-Jak activity. Furthermore, our data using epithelial organoid cultures suggest that at least a subset of IECs have paracrine or autocrine feed-forward mechanisms to produce and respond to one or more gp130-activating cytokines (*11*). Thus, our results suggest that the anti-tumor effect of Stat3 suppression was mediated by IEC-intrinsic

mechanisms and not the adaptive immune response, which can be reactivated in myeloid, dendritic, and natural killer cells in mice with systemic inhibition Stat3 (*44*).

Because the gp130-Jak-Stat3 and Wnt-β-catenin pathways promote the expression of common target genes, including *MYC* and *CCND1* (*45, 46*), it is possible that these pathways cooperate in tumor cells to induce transcription of these genes above a threshold required for cell proliferation. However, genetic or pharmacological inhibition of Stat3 did not reduce the accumulation of nuclear β-catenin or the expression of β-catenin target genes (*7*).

Our data suggested that Bmi-1 plays a role in controlling cell proliferation in intestinal cells with increased activation of β-catenin. *Bmi1* is overexpressed in various solid cancers (*47, 48*), including CRC (*49*), where increased *Bmi1* expression correlates with poor prognosis (*50*). Bmi-1 is a regulatory subunit of the polycomb repressor complex-1. In embryonic fibroblasts cells, BMI-1 represses transcription of *CDKN2A*, which encodes the cell cycle inhibitory proteins p16 and p14Arf (*39*). In mouse neural stem cells, Bmi-1 also represses expression of *Cdkn1A*, encoding the cell cycle inhibitor p21 (*51*). Knockdown of Bmi-1 causes cell cycle exit of cultured CRC cells with high Wnt-β-catenin signalling, but does not reduce the expression of Wnt-β-catenin target genes in these cells (*52*). Likewise, activation of β-catenin in *Bmi1* haploinsufficient mice only results in small intestinal adenomas (*53*). The latter observation is functionally compatible with a role of Bmi-1 in self-renewal of Lgr5+ intestinal stem cells (reviewed in (*54*).

Linking the proliferative capacity of intestinal crypts to a "gp130/Stat3 rheostat" appears phylogenetically conserved, as it is also required for regeneration of the fly mid-gut (*35*). In mammals, this enables the intestine to confine rapid mucosal regeneration to sites of greatest damage and hence greatest inflammation (*55*). This mechanism is reinforced by the capacity of the inflamed stroma to convert IEC through a NF-κB dependent mechanism to intestinal stem cells (*56*). Accordingly, homozygous $gp130^{\Delta Stat}$ mice display prolonged wounding of the intestinal mucosa and associated ulceration (*57*). Conversely, when the regenerative process is hijacked by *APC*- or β-catenin mutant cells, and irrespective of additional compounding mutations (e.g. *KRAS, TP53*), excessive STAT3 activity fuels the growth of the corresponding tumors. Accordingly, excessive STAT3 signaling is observed in a majority of human CRC (*58*). Here we provide comprehensive evidence that partial suppression of systemic gp130-Jak-Stat3 signaling is sufficient to limit tumor growth by reducing Bmi-1 dependent repression of p21 and p16 in models of familial inherited and sporadic CRC (Fig. 6G). Consistent with this model, intestinal tumorigenesis in fully gp130-Jak-Stat3 signaling-proficient *Apc*-mutant mice remains unaffected after ablation of p21 (*59*), because here we showed that in these situations p21 expression is already repressed through a Bmi-1-dependent mechanism.

A major obstacle to targeting Wnt-β-catenin signaling in cancer is the reliance of the intestinal epithelium on this pathway for renewal and regeneration. Tankyrase inhibitors, which promote degradation of β-catenin, have limited clinical utility for cancer because of toxicity associated with inhibition of IEC homeostasis (*60*). Other recent strategies have focused on mTorc1 (*61*), Notch (*62*), and components of other pathways that are not mutated in CRC but are rate-limiting for CRC proliferation. Clinical trials with gamma-secretase inhibitors, which block Notch

signaling, reveal gastrointestinal toxicity (*63*), whereas single agent therapies targeting the mTOR pathway conferred limited benefit (*64*). Here, we found that partial inhibition of gp130-Jak-Stat3 signaling selectively blocked proliferation of intestinal tumors driven by *APC*-mutations without perturbing intestinal homeostasis or causing the side-effects common in models using complete Stat3 ablation (*36, 65*). Therefore, our findings in mice provide proof of concept for the development of existing gp130-Jak-Stat3 pathway inhibitors as therapeutic modalities for CRC.

MATERIAL AND METHODS

Mice

All procedures involving animals were approved by the Ludwig Institute for Cancer Research Department of Surgery Animal Ethics Committee and the Walter and Eliza Hall Institute Animal Ethics Committee. The *gp130*$^{F/F}$, *gp130*$^{\Delta Stat/+}$, *Stat3*$^{+/-}$, *Apc*$^{Min/+}$ and *Lgr5*^{CreERT2}; *Apc*$^{fl/fl}$ mice have been descried previously (*12, 15, 57*) and compound *Apc*$^{Min/+}$; *gp130*$^{F/F}$, *Lgr5*^{CreERT2}; *Apc*$^{fl/fl}$; *gp130*$^{\Delta Stat/+}$ and *Apc*$^{Min/+}$; *gp130*$^{\Delta Stat/+}$ strains were derived from corresponding inter-crossings. *Lgr5*^{CreERT2}; *Apc*$^{fl/fl}$; *Stat3*$^{fl/+}$ and *Apc*$^{Min/+}$; *Bmi1*$^{+/-}$ mice were generated from *Stat3*$^{fl/fl}$ (*66*) and *Bmi1*$^{+/-}$ mice (*67*), respectively. All mice were co-housed and unless indicated, all mice were on an inbred C57BL/6 genetic background using appropriate littermates as controls. A single daily Tamoxifen injection occurred over 4 consecutive days with 3mg/mouse on day 1 and 2mg/mouse during the following days.

Irradiation induced regeneration

Adult mice were irradiated with a single dose of 14 Gy of γ-irradiation (0.414 Gy/min) and intestines were collected 72 hours later (*4*).

Tumor xenografts

Female BALB/c-nude mice were injected subcutaneously with 2x10^6 SW480 cells, or 5x10^6 DLD1, LIM1899 (*51*) and RKO cells. Cells were resuspended in Matrigel (BD Biosciences)/ PBS (1:1) to a final volume of 200 μl. Once tumors became palpable (>100 mm^3) approximately 5 days later, AZD1480 (30 mg/kg, Astra-Zeneca) was administered by daily oral gavage (*16*). BrdU was injected i.p. at 50mg/kg, 2h prior to tissue collection.

Histology

Mouse tissue collection and processing was carried out as previously detailed (*4*). Hematoxilin and Eosin-stained sections were scanned using an Aperio ScanScope XT (Aperio, USA) pathology slide scanner with a 20x PlanApo NA 0.6 objective and areas of interest were extracted using Aperio ImageScope software v11.1.2.760. Periodic Acid/Schiff stain was performed as described (*7*). Tumor burden was estimated by measuring the area covered by adenomas on histological cross-sections of rolled intestines using MetaMorph software v7.7.7, and then normalized to the length of the intestinal section on that slide (*24*).

Organoid Culture

Intestinal crypts from small intestines were harvested, washed and resuspended at 2000 crypts per ml of Matrigel (BD Biosciences) and 50 µl was then dispensed in each well of a 24-well plate. Once the Matrigel had set, serum-free culture medium was added, and the organoids were cultured for seven days as described (*18*). Organoid cultures were imaged on a Nikon Ti-E microscope using DIC contrast with a 10x PlanApo NA 0.3 objective. A focal stack of images was collected 10 µm apart and processed through the "Best Focus" function of MetaMorph v7.7.7 (Molecular Devices, USA) to generate the final image of individual organoids.

Tissue Culture and Soft Agar Colony Growth Assay

SW480 and SW480^{APC} cells (*33*) were seeded in 2 ml of RPMI media supplemented with 10 % FBS and 1 % penicillin/streptomycin in 35 mm culture dishes at a density of $2x10^5$ cells per dish. Three days later cultures were exposed to AZD1480 (2 µM) for 30 min. Co-immunofluorescence was then performed with antibodies to rabbit phospho-Stat3 (Tyr705, Santa Cruz #9134s, 1:200 dilution) and mouse β-catenin (Transduction Laboratories, 1:400).

Colony formation assays of SW480 cells in soft agar were performed as described (*33*) in the presence of methylcellulose (vehicle control), AZD1480 (2 μM), the Stat3 inhibitor S3I-201 (Biovision, 50 μM), epithelial growth factor receptor (EGFR) inhibitor AG1478 (Cell Signaling, 1μM), or recombinant human IL11 (Genetics Institute, 10 ng/ml) for 10 days.

Immunohistochemistry and Immunofluorescence

Tissues were fixed and immunohistochemistry performed as described previously (*7*). Primary antibodies used were rabbit phosphorylated Tyr^{705} Stat3 (Santa Cruz #9134s, 1:150), rabbit Thr^{202}/Tyr^{204} p42/44 MAPK (Cell Signaling #9101, 1:150), mouse β-catenin (Transduction Laboratories, 1:300), mouse BrdU (BD Biosciences, 1:300), rabbit PCNA (Santa Cruz #7907, 1:100), rabbit c-Myc (Santa Cruz #C1309, 1:200), rabbit Lysozyme (Neomarkers RB-372, 1:100) and goat p21 (Santa Cruz #Sc-397-G; 1:100). To assess the distribution of PCNA and β-catenin, we co-stained sections of mouse intestine using primary antibodies detailed above and fluorescent secondaries (rabbit IgG Alexa-488 for PCNA and mouse IgG Alexa-546 for β-catenin). Slides were tile scanned on a Nikon Ti-E microscope using a 10x PlanApo NA0.3 objective. The area of tumors was outlined manually to generate binary masks used to measure area, average intensity, shape factor, and intensity standard deviation of nuclei with MetaMorph v7.7.7. These values were assembled in Microsoft Excel and analysed with FlowJo .

Biochemical analysis

Gene expression analysis by reverse transcription and quantitative polymerase chain reaction (RT-qPCR) was performed using the SybrGreen method (ABI) as described (*17*). For RT-pPCR primer sequences please see Table S1. Fold change was calculated using the $2^{-\Delta\Delta CT}$ method (*68*).

Protein lysates were separated by SDS-PAGE and transferred to nitrocellulose. For Western blot analysis membranes were blocked in 5 % non-fat milk powder in PBS + 0.05% Tween-20 buffer and probed overnight with antibodies detecting p16 (Santa Cruz; #sc-467), Bmi-1 (Millipore; #05-637), Actin (Sigma; #A2066) or Gapdh (Santa Cruz; #sc-69778). All primary antibodies were diluted 1:1000 in 5% BSA (w/v) or 5% non-fat milk powder(w/v) in PBS + 0.05% Tween-20 buffer. Membranes were then incubated with an appropriate HRP-conjugated secondary antibody diluted at 1:3,000 in PBS + 0.05% Tween-20, for 2 hours at room temperature. Signals were visualized with a Chemidoc XRS+ (BioRad, Hercules, CA) chemiluminescence detection system.

For ChIP assays, 1×10^7 SW480 or SW480^{APC} cells were stimulated with IL11 (0.5 μg/ml) for 30 minutes. Chromatin was cross-linked with 1% formaldehyde for 10 minutes and sonicated to an average size of 400 base pairs using the Bioruptor Plus (Diagenode, Denville, USA). Immunoprecipitation was performed using Protein A Dynabeads (Life Technologies, Mulgrave, Australia). Each sample contained 10 μg of phosphorylated-STAT3 antibody (sc-482X, Santa Cruz Biotechnology, CA) or rabbit IgG (#02-6102, Life Technologies, Mulgrave, Australia). The crosslinks were reversed in 0.2 M NaCl in the presence of RNaseA (Life Technologies Mulgrave, Australia) at 65°C, over night. DNA fragments were purified using phenol chloroform extraction and ethanol precipitation. The immunopreciptated DNA was amplified by quantitative PCR using primers specific for intron1 of the *BMI-1* gene (forward: 5'-GCT GGA GGA CAA ATG GAA GA-3'; reverse: 5'-TGG GCT GTC CTA ACG TTT CT-3') and the *GAPDH* promoter (forward: 5'-TAC TAG CGG TTT TAC GGG CG-3'; reverse: 5'- TCG AAC AGG AGG AGC AGA GAG CGA-3').

Luciferase Reporter Assay

A 555 *bp* region around the predicted Stat3 binding site in the first intron of the murine *Bmi-1* gene (*40*) was amplified from genomic DNA using the forward primer 5'-AAG CTC GAG AGG GTT TAA GCA CCT TG-3' and reverse primer 5'-AAG TCT CCC AAA CCT GCA GCA ACT AT-3' and subcloned into pGL4_23 [luc2/minP] (Promega) to yield the *pBmi-1:luc* reporter plasmid. HEK293T cells were seeded in DMEM supplemented with 10 % FBS in 96 well plates at $1x10^4$ cells/well the day before transfection. The *pBmi-1:luc* and *pCMV-renilla* plasmids were co-transfected at a ratio of 40:1 using FuGENE 6 (Roche). Twenty-four hours later, cells were stimulated with the indicated concentrations of Hyper IL-6 (gift from S. Rose-John, Kiel, Germany) (*41*) for 4 hours. Luciferase activity was detected using the Dual-Luciferase Reporter Assay (Promega) and measured with a Lumistar Galaxy luminometer (Dynatech Laboratories). Luciferase assays using TOPFLASH were performed as described (*41*). Cells were treated with vehicle (DMSO), AZD1480 (2μM) or IL11 (10ng/ml) for 30 minutes before cell lysates were collected.

Supplementary Materials

Fig. S1 gp130-Jak-Stat3 signaling regulates intestinal regeneration and tumorigenesis.

Fig. S2 gp130-Jak-Stat3 signaling limits induced colonic tumorigenesis in in *Lgr5*^{CreERT2}; *Apc*$^{fl/fl}$ mice and human CRC xenografts.

Fig. S3 Gene signature for Wnt and gp130-Jak-Stat3 signaling co-exist in human colorectal cancers.

Fig S4 Xenograft growth is supressed by partial inhibition of the gp130-Jak-Stat3 pathway without effecting Stat1.

Fig. S5 Stimulation of gp130-Jak-Stat3 signaling does not affect aberrant Wnt-β-catenin signalling in the SW480 human CRC cell line.

Fig. S6 Inhibition of gp130-Jak-Stat3 signaling does not affect intestinal homeostasis.

Fig. S7 Inhibition of gp130-Jak-Stat3 signaling relieves Bmi1-mediated repression of the gene encoding p21 intestinal tumors.

Table S1 Primer sequences used for RT-qPRC

ACKNOWLEDGMENTS

We would like to thank S. Rose-John (Kiel, Germany) for the gift of Hyper IL-6, and Catherine Hall and David Vaux (Walter and Eliza Hall Institute, Australia) for assistance with xenograft experiments.

Funding: This work was supported by Ludwig Cancer Research, the Victorian State Government Operational Infrastructure Support, the IRIISS scheme of the National Health and Medical Research Council Australia (NHMRC), a grant from the Royal Melbourne Hospital #605030 (E.V, T.J.P), a grant from Cancer Council of Victoria #APP1020716 (E.V. and T.J.P)

and NHMRC grants #603127 (T.J.P, M.B), #566679 (E.V.), #487922 (M.E, R.G.R, M.B), #433617, #603122 (M.E) and #1064987 (T.J.P, M.B, M.E). M.E. and R.G.R. are NHMRC Senior Research Fellows.

AUTHOR CONTRIBUTIONS: T.J.P., M.B., and M.E. designed the study. T.J.P., M.B., E.S., S.S., D.J.F., M.F., H-H.Z., C.J.N., M.E., J.M. and H.B.P. performed experiments. F.W., R.G.G., V.P., O.S., D.K., D.H, A.W.B. and E.V. supervised specific experiments. R.J. and P.P. provided Bioinformatics analysis. T.J.P., M.B. and M.E. analyzed and interpreted data. T.J.P., M.B. and M.E. wrote the paper.

COMPETING FINANCIAL INTERESTS: D.H. has ownership interest (including patents) in AstraZeneca. T.J.P., M.B. E.S and M.E. filed a patent application for the use Jak inhibitors in treating colon cancer (Australia 2014-04-04PCT/AU2014/000370PCT, METHODS OF TREATING DISEASES CHARACTERIZED BY EXCESSIVE Wnt SIGNALING). All other authors declare no competing financial interests.

Data and Materials Availability: Mice, cells and AZD1480 are available by MTA as follows: *gp130*$^{F/F}$ and *gp130*$^{\Delta Stat/\Delta Stat}$ and the corresponding compound mutant mice:

M.E., The Walter and Eliza Hall Institute for Medical Research, Melbourne, Australia

SW480, SW480^{APC}, LIM1899 cell lines:

M.F., The Walter and Eliza Hall Institute for Medical Research, Melbourne, Australia

AZD1480:

D.H., AstraZeneca, Oncology iMed, Waltham, MA 02451, USA.

All other reagents are available either from commercial sources or open repositories

FIGURE LEGENDS

Fig. 1. Impaired gp130-Jak-Stat3 signaling supresses intestinal regeneration in response to irradiation and the growth of crypts in organoid culture.

A Immunohistochemical analysis for the proliferation marker PCNA on sections of small intestines collected 72h after γ-irradiation of mice of the indicated genotypes gavaged daily with AZD1480 (30 mg/kg) for 3 days prior to and 3 days after irradiation. Scale bar = 100 μm. The graph shows the quantification of intact, PCNA-positive crypts in cross sections from the proximal small intestine. Data are mean ± S.E.M of 3 mice per cohort. * $p \leq 0.04$. Mann-Whitney U-test. WT = wild-type.

B Immunohistochemical analysis for c-Myc and β-catenin on sections of small intestines from mice of the indicated genotype 72h after γ-irradiation. Regenerating crypts (black arrows) and non-regenerating epithelium (red arrows) are marked. Scale bar = 50 μm. Images are representative of 3 mice per cohort.

C Graph of the relative mRNA abundance for β-catenin target genes in IECs isolated from small intestines of wild-type and *gp130*$^{\Delta Stat/+}$ mice 72 h after γ-irradiation. Data are mean ± S.E.M. of 3 mice per cohort. * $p \leq 0.04$. Mann-Whitney U-test.

D Representative organoids grown from crypts of the small intestines of *gp130*$^{F/F}$ or WT mice or from WT mice and cultured in the presence of the Stat3 inhibitor S3I-201 (Stat3i, 7.5 μM) from day 3 after seeding. Arrows point to budding crypt-like structures. Scale bar = 50 μm. The graph shows the quantification of budding crypt-like structures on individual

organoids. Crypts per organoid were counted for every organoid in a 10x field of view over a 5 day period. Data are mean ± SD. N=2.

Fig. 2. gp130-Jak-Stat3 signaling is rate-limiting during spontaneous intestinal tumorigenesis in *Apc*$^{Min/+}$ mice.

A Quantification of number and size of tumors in the small intestines and colon of 150 day old *Apc*$^{Min/+}$ and *Apc*$^{Min/+}$; *gp130*$^{\Delta Stat/+}$ mice. Data are mean ± S.E.M. of 8 mice per cohort. * $p \leq 0.002$. Mann-Whitney U-test.

B Representative images of emerging colonic tumors labelled with methylene blue in 100 day old mice of the indicated genotypes. Scale bar = 500 μm. The graphs show quantification of the number and area of intestinal tumors. Data are mean ± S.E.M. of 5 mice per cohort. * $p \leq 0.02$. Mann-Whitney U-test.

C Quantification of the number and area of intestinal tumors in mice of the indicated genotypes. Data are mean ± S.E.M. of 5 mice per cohort. * $p \leq 0.02$. Mann-Whitney U-test.

Fig. 3. gp130-Jak-Stat3 signaling is rate-limiting during induced intestinal tumorigenesis in *Lgr5*^{CreERT2}*; Apc*$^{fl/fl}$ mice.

A Representative images of haematoxylin- and eosin-stained cross-sections of small intestines from mice of the indicated genotypes and collected 35 days after tamoxifen administration. Neoplastic foci (microadenoma) are indicated by arrowheads and tubular adenomas are indicated by arrows. Scale bars = 1mm. The graphs show the quantification of the cross-sectional area of intestinal tumors. Data were normalized for the length of the intestine on

the section analysed and represent the mean ± S.E.M. of 3 mice per cohort. * $p \leq 0.04$. Mann-Whitney U-test.

B Immunofluorescence staining for β-catenin and PCNA in sections of intestinal tumors from adult mice of the indicated genotype 35 days after tamoxifen administration. Scale bar = 50 μm. The graph shows the quantification of β-catenin and PCNA labelled epithelial cells in tumors. Data were normalized for the total number of tumor-associated IECs using DAPI-stained nuclei as reference and represent the mean ± S.E.M. of 3 mice per cohort. * $p \leq 0.04$. Mann-Whitney U-test.

Fig. 4. AZD1480 limits intestinal tumorigenesis in in *Lgr5*^{CreERT2}*; Apc*$^{fl/fl}$ and *Apc*^{Min} mice.

A Representative images of haematoxylin- and eosin-stained cross-sections of small intestine from *Lgr5*^{CreERT2}; *Apc*$^{fl/fl}$ mice and collected 35 days after tamoxifen administration and daily gavages with AZD1480 (30 mg/kg) or vehicle. Neoplastic foci (microadenoma) are indicated by arrowheads and tubular adenomas are indicated by arrows. Scale bars = 1mm. The graphs show the quantification of the cross-sectional area of intestinal tumors. Data were normalized for the length of the intestine on the section analysed and represent the mean ± S.E.M. of 3 mice per cohort. * $p \leq 0.04$. Mann-Whitney U-test.

B Enumeration of total number and size of intestinal tumors in individual *Apc*^{Min} mice at 6 weeks of age and 12 weeks of age following treatment with daily gavages of AZD1480 (30 mg/kg) or vehicle for the last 6 weeks. NSD = not significantly different. Data represent the mean ± S.E.M. of 3 mice per cohort. * $p \leq 0.04$. Mann-Whitney U-test.

Fig. 5. Inhibition of gp130-Jak-Stat3 signaling blocks tumor growth in human CRC cells with activating mutations in the Wnt-β-catenin pathway.

A Graphs of the volume of tumor xenografts in BALB/c-nude mice injected subcutaneously with the indicated human CRC cell lines and gavaged daily with AZD1480 (30 mg/kg, daily) or vehicle starting on the 5^{th} day after cell injection. Data are mean ± S.E.M. of 8 tumors per condition. * $p \leq 0.039$. Student's t-test. NSD = not significantly different.

B Representative photograph of SW480 and SW480^{APC} CRC cells grown for 10 days under colony forming conditions in soft agar in the presence of AZD1480 (2 μM) or vehicle. Scale bar = 200 μm. The graph shows the quantification of normalized number of colonies containing >50 cells. Data are mean ± S.E.M. of triplicate cultures from 3 independent experiments. * $p \leq 0.04$. Mann-Whitney U-test.

Fig. 6. Inhibition of gp130-Jak-Stat3 signaling promotes cell cycle inhibition through Bmi1.

A Graph of the relative mRNA abundance for the indicated genes in SW480 xenografts from mice that were gavaged daily for 35 days with AZD1480 (30mg/kg, daily) or vehicle control. Data are mean ± S.E.M. of 3 mice per condition. * $p \leq 0.04$. Mann-Whitney U-test.

B Western blot analysis for p16 in intestinal tumors of 18 week old mice of the indicated genotypes. Gapdh was used as loading control. Each lane represents an individual mouse.

C Immunohistochemical analysis of p21 in intestinal tumors of 18 week old mice of the indicated genotypes. Scale bar = 100μm. Images are representative of 3 mice per genotype.

D **I**mmunohistochemical analysis of p21 in SW480 CRC xenografts resected from mice that were gavaged daily for 35 days with AZD1480 (30mg/kg, daily) or vehicle control. Scale bar = 100μm. Images are representative of 3 mice.

E Graph of the relative enrichment of the indicated loci using ChIP with antibodies targeting IgG or phosphorylated Tyr^{205} Stat3 and lysates from SW480 cells exposed to IL11 (500ng/ml) or PBS for 30 minutes. Data are mean ± S.E.M. of 3 independent experiments. * $p < 0.04$. Student's *t*-test.

F Quantification of the number of tumors in the small intestine of 18 week old $Apc^{Min/+}$ or $Apc^{Min/+}$; $Bmi1^{+/-}$ mice. Data are mean ± S.E.M. of 3 mice per cohort. * $p \leq 0.04$. Mann-Whitney U-test.

G Schematic representation showing how the gp130-Jak-Stat3-Bmi-1 pathway acts as a rheostat to regulate Wnt-β-catenin activated cell proliferation (Apc* = mutated Apc).

REFERENCES

1. H. Clevers, The intestinal crypt, a prototype stem cell compartment. *Cell* 154, 274-284 (2013).
2. H. Ireland, R. Kemp, C. Houghton, L. Howard, A. R. Clarke, O. J. Sansom, D. J. Winton, Inducible Cre-mediated control of gene expression in the murine gastrointestinal tract: effect of loss of beta-catenin. *Gastroenterology* 126, 1236-1246 (2004).
3. V. Muncan, O. J. Sansom, L. Tertoolen, T. J. Phesse, H. Begthel, E. Sancho, A. M. Cole, A. Gregorieff, I. M. de Alboran, H. Clevers, A. R. Clarke, Rapid loss of intestinal crypts upon conditional deletion of the Wnt/Tcf-4 target gene c-Myc. *Mol Cell Biol* 26, 8418-8426 (2006).
4. G. H. Ashton, J. P. Morton, K. Myant, T. J. Phesse, R. A. Ridgway, V. Marsh, J. A. Wilkins, D. Athineos, V. Muncan, R. Kemp, K. Neufeld, H. Clevers, V. Brunton, D. J. Winton, X. Wang, R. C. Sears, A. R. Clarke, M. C. Frame, O. J. Sansom, Focal adhesion kinase is required for intestinal regeneration and tumorigenesis downstream of Wnt/c-Myc signaling. *Dev Cell* 19, 259-269 (2010).
5. H. Clevers, R. Nusse, Wnt/beta-catenin signaling and disease. *Cell* 149, 1192-1205 (2012).
6. J. N. Anastas, R. T. Moon, WNT signalling pathways as therapeutic targets in cancer. *Nature Reviews* 13, 11-26 (2013).
7. O. J. Sansom, V. S. Meniel, V. Muncan, T. J. Phesse, J. A. Wilkins, K. R. Reed, J. K. Vass, D. Athineos, H. Clevers, A. R. Clarke, Myc deletion rescues Apc deficiency in the small intestine. *Nature* 446, 676-679 (2007).
8. L. Soucek, J. Whitfield, C. P. Martins, A. J. Finch, D. J. Murphy, N. M. Sodir, A. N. Karnezis, L. B. Swigart, S. Nasi, G. I. Evan, Modelling Myc inhibition as a cancer therapy. *Nature* 455, 679-683 (2008).
9. A. Jarnicki, T. Putoczki, M. Ernst, Stat3: linking inflammation to epithelial cancer - more than a "gut" feeling? *Cell Div* 5, 14 (2010).
10. M. Ernst, T. Putoczki, Molecular Pathways: IL11 as a Tumor-Promoting Cytokine-Translational Implications for Cancers. *Clin Cancer Res.*, (2014).
11. T. L. Putoczki, S. Thiem, A. Loving, R. A. Busuttil, N. J. Wilson, P. K. Ziegler, P. M. Nguyen, A. Preaudet, R. Farid, K. M. Edwards, Y. Boglev, R. B. Luwor, A. Jarnicki, D. Horst, A. Boussioutas, J. K. Heath, O. M. Sieber, I. Pleines, B. T. Kile, A. Nash, F. R. Greten, B. S. McKenzie, M. Ernst, Interleukin-11 is the dominant IL-6 family cytokine during gastrointestinal tumorigenesis and can be targeted therapeutically. *Cancer Cell* 24, 257-271 (2013).
12. N. C. Tebbutt, A. S. Giraud, M. Inglese, B. Jenkins, P. Waring, F. J. Clay, S. Malki, B. M. Alderman, D. Grail, F. Hollande, J. K. Heath, M. Ernst, Reciprocal regulation of gastrointestinal homeostasis by SHP2 and STAT-mediated trefoil gene activation in gp130 mutant mice. *Nature Medicine* 8, 1089-1097 (2002).
13. J. Bollrath, T. J. Phesse, V. A. von Burstin, T. Putoczki, M. Bennecke, T. Bateman, T. Nebelsiek, T. Lundgren-May, O. Canli, S. Schwitalla, V. Matthews, R. M. Schmid, T. Kirchner, M. C. Arkan, M. Ernst, F. R. Greten, gp130-mediated Stat3 activation in

enterocytes regulates cell survival and cell-cycle progression during colitis-associated tumorigenesis. *Cancer Cell* 15, 91-102 (2009).
14. T. Kusaba, T. Nakayama, K. Yamazumi, Y. Yakata, A. Yoshizaki, T. Nagayasu, I. Sekine, Expression of p-STAT3 in human colorectal adenocarcinoma and adenoma; correlation with clinicopathological factors. *Journal of Clinical Pathology* 58, 833-838 (2005).
15. K. Takeda, K. Noguchi, W. Shi, T. Tanaka, M. Matsumoto, N. Yoshida, T. Kishimoto, S. Akira, Targeted disruption of the mouse Stat3 gene leads to early embryonic lethality. *Proc Natl Acad Sci U S A* 94, 3801-3804 (1997).
16. M. Hedvat, D. Huszar, A. Herrmann, J. M. Gozgit, A. Schroeder, A. Sheehy, R. Buettner, D. Proia, C. M. Kowolik, H. Xin, B. Armstrong, G. Bebernitz, S. Weng, L. Wang, M. Ye, K. McEachern, H. Chen, D. Morosini, K. Bell, M. Alimzhanov, S. Ioannidis, P. McCoon, Z. A. Cao, H. Yu, R. Jove, M. Zinda, The JAK2 inhibitor AZD1480 potently blocks Stat3 signaling and oncogenesis in solid tumors. *Cancer Cell* 16, 487-497 (2009).
17. T. J. Phesse, L. Parry, K. R. Reed, K. B. Ewan, T. C. Dale, O. J. Sansom, A. R. Clarke, Deficiency of Mbd2 attenuates Wnt signaling. *Mol Cell Biol* 28, 6094-6103 (2008).
18. T. Sato, J. H. van Es, H. J. Snippert, D. E. Stange, R. G. Vries, M. van den Born, N. Barker, N. F. Shroyer, M. van de Wetering, H. Clevers, Paneth cells constitute the niche for Lgr5 stem cells in intestinal crypts. *Nature* 469, 415-418 (2011).
19. K. Siddiquee, S. Zhang, W. C. Guida, M. A. Blaskovich, B. Greedy, H. R. Lawrence, M. L. Yip, R. Jove, M. M. McLaughlin, N. J. Lawrence, S. M. Sebti, J. Turkson, Selective chemical probe inhibitor of Stat3, identified through structure-based virtual screening, induces antitumor activity. *Proc Natl Acad Sci U S A* 104, 7391-7396 (2007).
20. L. K. Su, K. W. Kinzler, B. Vogelstein, A. C. Preisinger, A. R. Moser, C. Luongo, K. A. Gould, W. F. Dove, Multiple intestinal neoplasia caused by a mutation in the murine homolog of the APC gene. *Science* 256, 668-670 (1992).
21. M. Musteanu, L. Blaas, M. Mair, M. Schlederer, M. Bilban, S. Tauber, H. Esterbauer, M. Mueller, E. Casanova, L. Kenner, V. Poli, R. Eferl, Stat3 is a negative regulator of intestinal tumor progression in Apc(Min) mice. *Gastroenterology* 138, 1003-1011 e1001-1005 (2010).
22. E. A. McLellan, R. P. Bird, Aberrant crypts: potential preneoplastic lesions in the murine colon. *Cancer Res* 48, 6187-6192 (1988).
23. B. J. Shields, C. Hauser, P. E. Bukczynska, N. W. Court, T. Tiganis, DNA replication stalling attenuates tyrosine kinase signaling to suppress S phase progression. *Cancer Cell* 14, 166-179 (2008).
24. N. Barker, R. A. Ridgway, J. H. van Es, M. van de Wetering, H. Begthel, M. van den Born, E. Danenberg, A. R. Clarke, O. J. Sansom, H. Clevers, Crypt stem cells as the cells-of-origin of intestinal cancer. *Nature* 457, 608-611 (2009).
25. H. Yu, D. Pardoll, R. Jove, STATs in cancer inflammation and immunity: a leading role for STAT3. *Nature Reviews* 9, 798-809 (2009).
26. S. Verstovsek, R. A. Mesa, J. Gotlib, R. S. Levy, V. Gupta, J. F. DiPersio, J. V. Catalano, M. Deininger, C. Miller, R. T. Silver, M. Talpaz, E. F. Winton, J. H. Harvey, Jr., M. O. Arcasoy, E. Hexner, R. M. Lyons, R. Paquette, A. Raza, K. Vaddi, S. Erickson-Viitanen, I. L. Koumenis, W. Sun, V. Sandor, H. M. Kantarjian, A double-blind, placebo-controlled trial of ruxolitinib for myelofibrosis. *N Engl J Med* 366, 799-807 (2012).

27. Y. Hong, T. Downey, K. W. Eu, P. K. Koh, P. Y. Cheah, A 'metastasis-prone' signature for early-stage mismatch-repair proficient sporadic colorectal cancer patients and its implications for possible therapeutics. *Clinical & Experimental Metastasis* 27, 83-90 (2010).
28. M. Skrzypczak, K. Goryca, T. Rubel, A. Paziewska, M. Mikula, D. Jarosz, J. Pachlewski, J. Oledzki, J. Ostrowski, Modeling oncogenic signaling in colon tumors by multidirectional analyses of microarray data directed for maximization of analytical reliability. *PLoS ONE* 5, (2010).
29. W. de Lau, N. Barker, T. Y. Low, B. K. Koo, V. S. Li, H. Teunissen, P. Kujala, A. Haegebarth, P. J. Peters, M. van de Wetering, D. E. Stange, J. E. van Es, D. Guardavaccaro, R. B. Schasfoort, Y. Mohri, K. Nishimori, S. Mohammed, A. J. Heck, H. Clevers, Lgr5 homologues associate with Wnt receptors and mediate R-spondin signalling. *Nature* 476, 293-297 (2011).
30. Y. M. Oh, J. K. Kim, Y. Choi, S. Choi, J. Y. Yoo, Prediction and experimental validation of novel STAT3 target genes in human cancer cells. *PLoS ONE* 4, e6911 (2009).
31. M. Snyder, X. Y. Huang, J. J. Zhang, Identification of novel direct Stat3 target genes for control of growth and differentiation. *J Biol Chem* 283, 3791-3798 (2008).
32. A. P. Costa-Pereira, S. Tininini, B. Strobl, T. Alonzi, J. F. Schlaak, H. Is'harc, I. Gesualdo, S. J. Newman, I. M. Kerr, V. Poli, Mutational switch of an IL-6 response to an interferon-gamma-like response. *Proc Natl Acad Sci U S A* 99, 8043-8047 (2002).
33. M. C. Faux, J. L. Ross, C. Meeker, T. Johns, H. Ji, R. J. Simpson, M. J. Layton, A. W. Burgess, Restoration of full-length adenomatous polyposis coli (APC) protein in a colon cancer cell line enhances cell adhesion. *Journal of Cell Science* 117, 427-439 (2004).
34. R. Radinsky, S. Risin, D. Fan, Z. Dong, D. Bielenberg, C. D. Bucana, I. J. Fidler, Level and function of epidermal growth factor receptor predict the metastatic potential of human colon carcinoma cells. *Clinical Cancer Research* 1, 19-31 (1995).
35. J. B. Cordero, R. K. Stefanatos, K. Myant, M. Vidal, O. J. Sansom, Non-autonomous crosstalk between the Jak/Stat and Egfr pathways mediates Apc1-driven intestinal stem cell hyperplasia in the Drosophila adult midgut. *Development* 139, 4524-4535 (2012).
36. J. R. Matthews, O. J. Sansom, A. R. Clarke, Absolute requirement for STAT3 function in small-intestine crypt stem cell survival. *Cell Death and Differentiation*, (2011).
37. J. F. McManus, Histological demonstration of mucin after periodic acid. *Nature* 158, 202 (1946).
38. T. Peeters, G. Vantrappen, The Paneth cell: a source of intestinal lysozyme. *Gut* 16, 553-558 (1975).
39. A. P. Bracken, D. Kleine-Kohlbrecher, N. Dietrich, D. Pasini, G. Gargiulo, C. Beekman, K. Theilgaard-Monch, S. Minucci, B. T. Porse, J. C. Marine, K. H. Hansen, K. Helin, The Polycomb group proteins bind throughout the INK4A-ARF locus and are disassociated in senescent cells. *Genes Dev* 21, 525-530 (2007).
40. F. Vallania, D. Schiavone, S. Dewilde, E. Pupo, S. Garbay, R. Calogero, M. Pontoglio, P. Provero, V. Poli, Genome-wide discovery of functional transcription factor binding sites by comparative genomics: the case of Stat3. *Proc Natl Acad Sci U S A* 106, 5117-5122 (2009).
41. M. Ernst, M. Najdovska, D. Grail, T. Lundgren-May, M. Buchert, H. Tye, V. B. Matthews, J. Armes, P. S. Bhathal, N. R. Hughes, E. G. Marcusson, J. G. Karras, S. Na, J. D. Sedgwick, P. J. Hertzog, B. J. Jenkins, STAT3 and STAT1 mediate IL-11-

dependent and inflammation-associated gastric tumorigenesis in gp130 receptor mutant mice. *Journal of Clinical Cnvestigation* 118, 1727-1738 (2008).
42. K. Brocke-Heidrich, B. Ge, H. Cvijic, G. Pfeifer, D. Loffler, C. Henze, T. W. McKeithan, F. Horn, BCL3 is induced by IL-6 via Stat3 binding to intronic enhancer HS4 and represses its own transcription. *Oncogene* 25, 7297-7304 (2006).
43. O. J. Sansom, V. Meniel, J. A. Wilkins, A. M. Cole, K. A. Oien, V. Marsh, T. J. Jamieson, C. Guerra, G. H. Ashton, M. Barbacid, A. R. Clarke, Loss of Apc allows phenotypic manifestation of the transforming properties of an endogenous K-ras oncogene in vivo. *Proc Natl Acad Sci U S A* 103, 14122-14127 (2006).
44. M. Kortylewski, M. Kujawski, T. Wang, S. Wei, S. Zhang, S. Pilon-Thomas, G. Niu, H. Kay, J. Mule, W. G. Kerr, R. Jove, D. Pardoll, H. Yu, Inhibiting Stat3 signaling in the hematopoietic system elicits multicomponent antitumor immunity. *Nature Medicine* 11, 1314-1321 (2005).
45. O. J. Sansom, K. R. Reed, A. J. Hayes, H. Ireland, H. Brinkmann, I. P. Newton, E. Batlle, P. Simon-Assmann, H. Clevers, I. S. Nathke, A. R. Clarke, D. J. Winton, Loss of Apc in vivo immediately perturbs Wnt signaling, differentiation, and migration. *Genes Dev* 18, 1385-1390 (2004).
46. B. J. Jenkins, D. Grail, T. Nheu, M. Najdovska, B. Wang, P. Waring, M. Inglese, R. M. McLoughlin, S. A. Jones, N. Topley, H. Baumann, L. M. Judd, A. S. Giraud, A. Boussioutas, H. J. Zhu, M. Ernst, Hyperactivation of Stat3 in gp130 mutant mice promotes gastric hyperproliferation and desensitizes TGF-beta signaling. *Nature Medicine* 11, 845-852 (2005).
47. Y. Q. Tong, B. Liu, H. Y. Zheng, Y. J. He, J. Gu, F. Li, Y. Li, Overexpression of BMI-1 is associated with poor prognosis in cervical cancer. *Asia-Pacific Journal of Clinical Oncology* 8, e55-62 (2012).
48. T. Yin, H. Wei, Z. Leng, Z. Yang, S. Gou, H. Wu, G. Zhao, X. Hu, C. Wang, Bmi-1 promotes the chemoresistance, invasion and tumorigenesis of pancreatic cancer cells. *Chemotherapy* 57, 488-496 (2011).
49. D. W. Li, H. M. Tang, J. W. Fan, D. W. Yan, C. Z. Zhou, S. X. Li, X. L. Wang, Z. H. Peng, Expression level of Bmi-1 oncoprotein is associated with progression and prognosis in colon cancer. *Journal of Cancer Research and Clinical Oncology* 136, 997-1006 (2010).
50. J. Du, Y. Li, J. Li, J. Zheng, Polycomb group protein Bmi1 expression in colon cancers predicts the survival. *Med Oncol* 27, 1273-1276 (2010).
51. C. A. Fasano, J. T. Dimos, N. B. Ivanova, N. Lowry, I. R. Lemischka, S. Temple, shRNA knockdown of Bmi-1 reveals a critical role for p21-Rb pathway in NSC self-renewal during development. *Cell Stem Cell* 1, 87-99 (2007).
52. A. Kreso, P. van Galen, N. M. Pedley, E. Lima-Fernandes, C. Frelin, T. Davis, L. Cao, R. Baiazitov, W. Du, N. Sydorenko, Y. C. Moon, L. Gibson, Y. Wang, C. Leung, N. N. Iscove, C. H. Arrowsmith, E. Szentgyorgyi, S. Gallinger, J. E. Dick, C. A. O'Brien, Self-renewal as a therapeutic target in human colorectal cancer. *Nature Medicine* 20, 29-36 (2014).
53. E. Sangiorgi, M. R. Capecchi, Bmi1 is expressed in vivo in intestinal stem cells. *Nat Genet* 40, 915-920 (2008).
54. N. Barker, Adult intestinal stem cells: critical drivers of epithelial homeostasis and regeneration. *Nature Reviews. Mol Cell Biol* 15, 19-33 (2014).

55. R. M. Logan, A. M. Stringer, J. M. Bowen, A. S. Yeoh, R. J. Gibson, S. T. Sonis, D. M. Keefe, The role of pro-inflammatory cytokines in cancer treatment-induced alimentary tract mucositis: pathobiology, animal models and cytotoxic drugs. *Cancer Treatment Reviews* 33, 448-460 (2007).
56. S. Schwitalla, A. A. Fingerle, P. Cammareri, T. Nebelsiek, S. I. Goktuna, P. K. Ziegler, O. Canli, J. Heijmans, D. J. Huels, G. Moreaux, R. A. Rupec, M. Gerhard, R. Schmid, N. Barker, H. Clevers, R. Lang, J. Neumann, T. Kirchner, M. M. Taketo, G. R. van den Brink, O. J. Sansom, M. C. Arkan, F. R. Greten, Intestinal tumorigenesis initiated by dedifferentiation and acquisition of stem-cell-like properties. *Cell* 152, 25-38 (2013).
57. M. Ernst, M. Inglese, P. Waring, I. K. Campbell, S. Bao, F. J. Clay, W. S. Alexander, I. P. Wicks, D. M. Tarlinton, U. Novak, J. K. Heath, A. R. Dunn, Defective gp130-mediated signal transducer and activator of transcription (STAT) signaling results in degenerative joint disease, gastrointestinal ulceration, and failure of uterine implantation. *Journal of Experimental Medicine* 194, 189-203 (2001).
58. T. Morikawa, Y. Baba, M. Yamauchi, A. Kuchiba, K. Nosho, K. Shima, N. Tanaka, C. Huttenhower, D. A. Frank, C. S. Fuchs, S. Ogino, STAT3 expression, molecular features, inflammation patterns, and prognosis in a database of 724 colorectal cancers. *Clinical Cancer Research* 17, 1452-1462 (2011).
59. A. M. Cole, R. A. Ridgway, S. E. Derkits, L. Parry, N. Barker, H. Clevers, A. R. Clarke, O. J. Sansom, p21 loss blocks senescence following Apc loss and provokes tumourigenesis in the renal but not the intestinal epithelium. *EMBO Molecular Medicine* 2, 472-486 (2010).
60. T. Lau, E. Chan, M. Callow, J. Waaler, J. Boggs, R. A. Blake, S. Magnuson, A. Sambrone, M. Schutten, R. Firestein, O. Machon, V. Korinek, E. Choo, D. Diaz, M. Merchant, P. Polakis, D. D. Holsworth, S. Krauss, M. Costa, A novel tankyrase small-molecule inhibitor suppresses APC mutation-driven colorectal tumor growth. *Cancer Res* 73, 3132-3144 (2013).
61. T. Fujishita, K. Aoki, H. A. Lane, M. Aoki, M. M. Taketo, Inhibition of the mTORC1 pathway suppresses intestinal polyp formation and reduces mortality in ApcDelta716 mice. *Proc Natl Acad Sci U S A* 105, 13544-13549 (2008).
62. J. H. van Es, M. E. van Gijn, O. Riccio, M. van den Born, M. Vooijs, H. Begthel, M. Cozijnsen, S. Robine, D. J. Winton, F. Radtke, H. Clevers, Notch/gamma-secretase inhibition turns proliferative cells in intestinal crypts and adenomas into goblet cells. *Nature* 435, 959-963 (2005).
63. J. R. Strosberg, T. Yeatman, J. Weber, D. Coppola, M. J. Schell, G. Han, K. Almhanna, R. Kim, T. Valone, H. Jump, D. Sullivan, A phase II study of RO4929097 in metastatic colorectal cancer. *Eur J Cancer* 48, 997-1003 (2012).
64. J. Rodon, R. Dienstmann, V. Serra, J. Tabernero, Development of PI3K inhibitors: lessons learned from early clinical trials. *Nature Reviews. Clinical oncology* 10, 143-153 (2013).
65. S. G. Tangye, M. C. Cook, D. A. Fulcher, Insights into the role of STAT3 in human lymphocyte differentiation as revealed by the hyper-IgE syndrome. *J Immunol* 182, 21-28 (2009).
66. T. Alonzi, D. Maritano, B. Gorgoni, G. Rizzuto, C. Libert, V. Poli, Essential role of STAT3 in the control of the acute-phase response as revealed by inducible gene inactivation [correction of activation] in the liver. *Mol Cell Biol* 21, 1621-1632 (2001).

67. N. M. van der Lugt, J. Domen, K. Linders, M. van Roon, E. Robanus-Maandag, H. te Riele, M. van der Valk, J. Deschamps, M. Sofroniew, M. van Lohuizen, et al., Posterior transformation, neurological abnormalities, and severe hematopoietic defects in mice with a targeted deletion of the bmi-1 proto-oncogene. *Genes Dev* 8, 757-769 (1994).
68. K. J. Livak, T. D. Schmittgen, Analysis of relative gene expression data using real-time quantitative PCR and the 2(-Delta Delta C(T)) Method. *Methods* 25, 402-408 (2001).

Figure 1

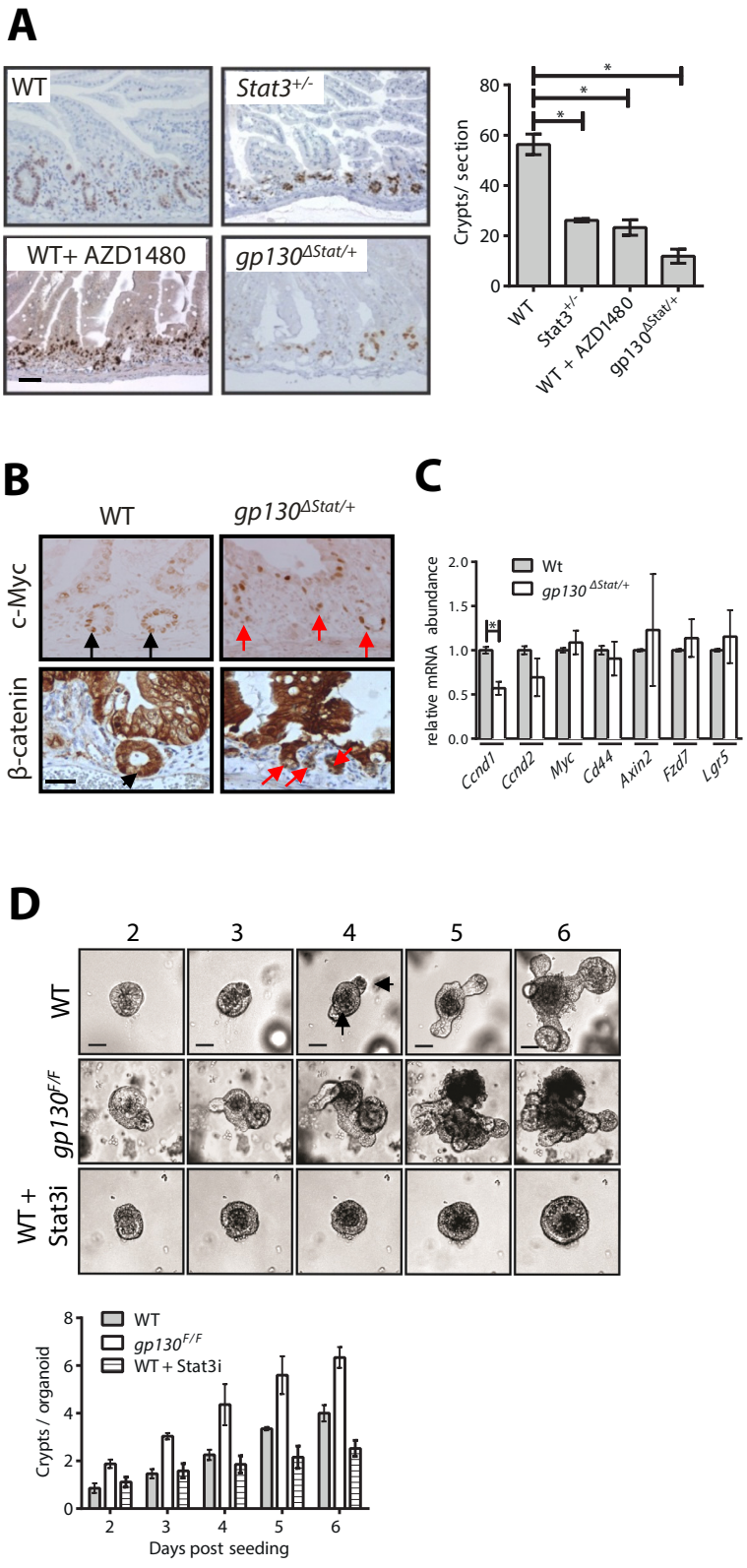
A
WT
Stat3+/-
WT+ AZD1480
gp130ΔStat/+
Crypts/ section
80
60
40
20
0
*
*
*
WT
Stat3+/-
WT + AZD1480
gp130ΔStat/+
B
WT
gp130ΔStat/+
c-Myc
β-catenin
C
Wt
gp130 ΔStat/+
relative mRNA abundance
2.0
1.5
1.0
0.5
0.0
*
Ccnd1
Ccnd2
Myc
Cd44
Axin2
Fzd7
Lgr5
D
2
3
4
5
6
WT
gp130F/F
WT + Stat3i
WT
gp130F/F
WT + Stat3i
Crypts / organoid
8
6
4
2
0
2
3
4
5
6
Days post seeding

Figure 2

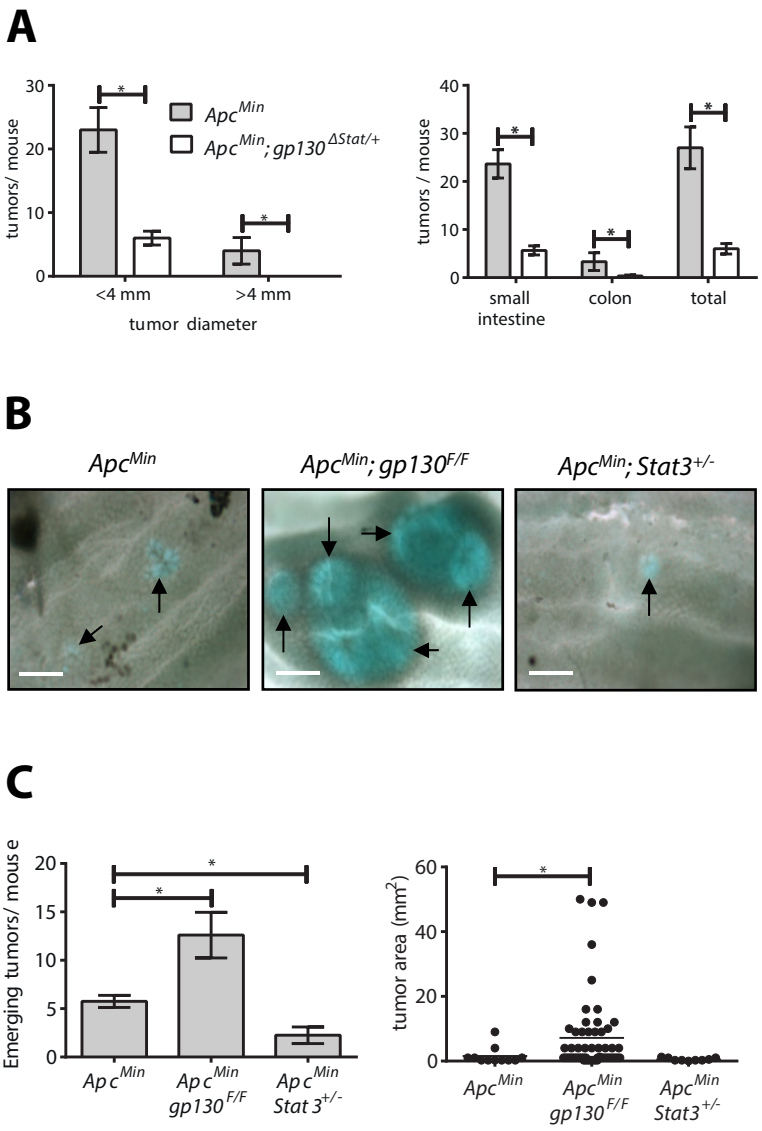
A
tumors/ mouse
Apc^Min
Apc^Min; gp130^ΔStat/+
<4 mm
>4 mm
tumor diameter
tumors / mouse
small intestine
colon
total
B
Apc^Min
Apc^Min; gp130^F/F
Apc^Min; Stat3^+/-
C
Emerging tumors/ mouse
Apc^Min
Apc^Min gp130^F/F
Apc^Min Stat3^+/-
tumor area (mm^2)

Figure 3

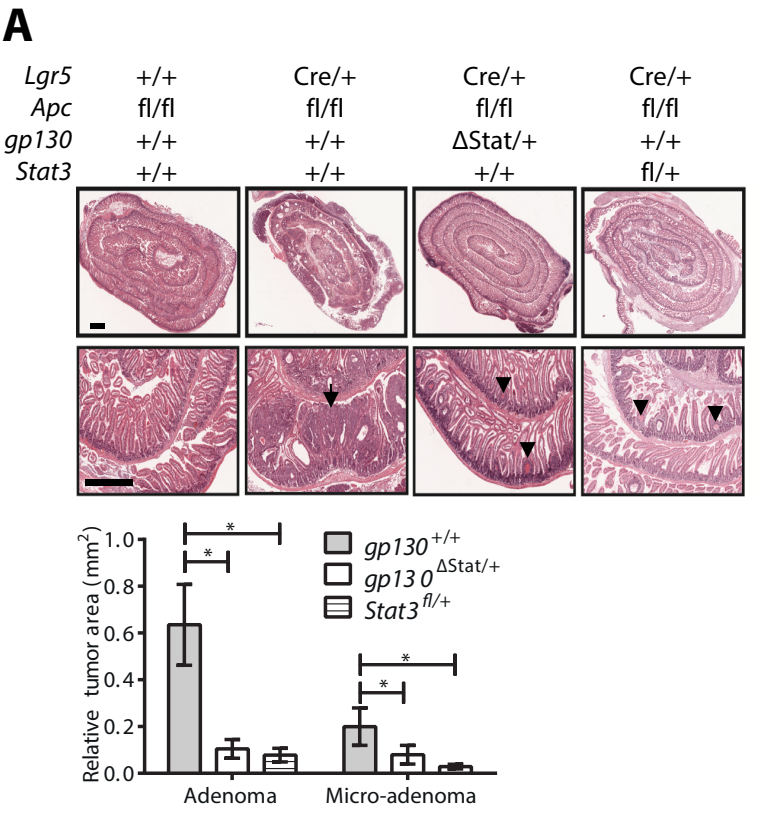
A
Lgr5 +/+ Cre/+ Cre/+ Cre/+
Apc fl/fl fl/fl fl/fl fl/fl
gp130 +/+ +/+ ΔStat/+ +/+
Stat3 +/+ +/+ +/+ fl/+
Relative tumor area (mm2)
1.0
0.8
0.6
0.4
0.2
0.0
gp130+/+
gp130ΔStat/+
Stat3fl/+
Adenoma
Micro-adenoma

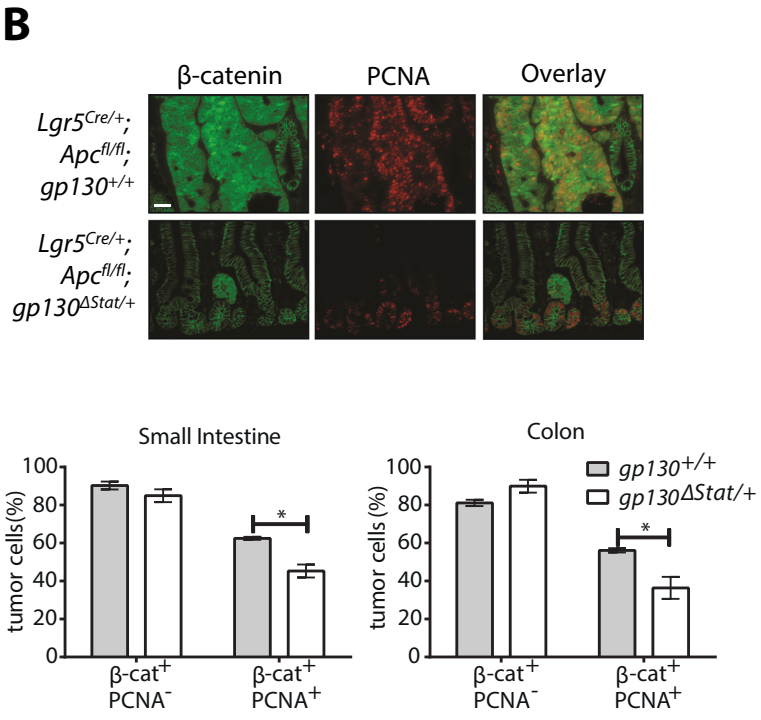
B
β-catenin
PCNA
Overlay
Lgr5Cre/+; Apcfl/fl; gp130+/+
Lgr5Cre/+; Apcfl/fl; gp130ΔStat/+
Small Intestine
Colon
tumor cells(%)
100
80
60
40
20
0
gp130+/+
gp130ΔStat/+
β-cat+ PCNA-
β-cat+ PCNA+

Figure 4

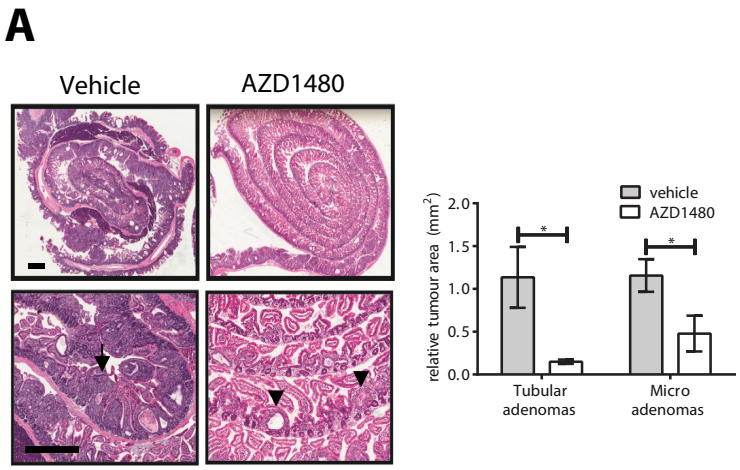
A
Vehicle
AZD1480
relative tumour area (mm2)
2.0
1.5
1.0
0.5
0.0
vehicle
AZD1480
*
*
Tubular adenomas
Micro adenomas
B
NSD
*
*
tumors/ mouse
80
60
40
20
0
NSD
*
*
tumor area/ mouse (mm2)
80
60
40
20
0
6w old
12w old following 6w vehicle
12w old following 6w AZD1480

Figure 5

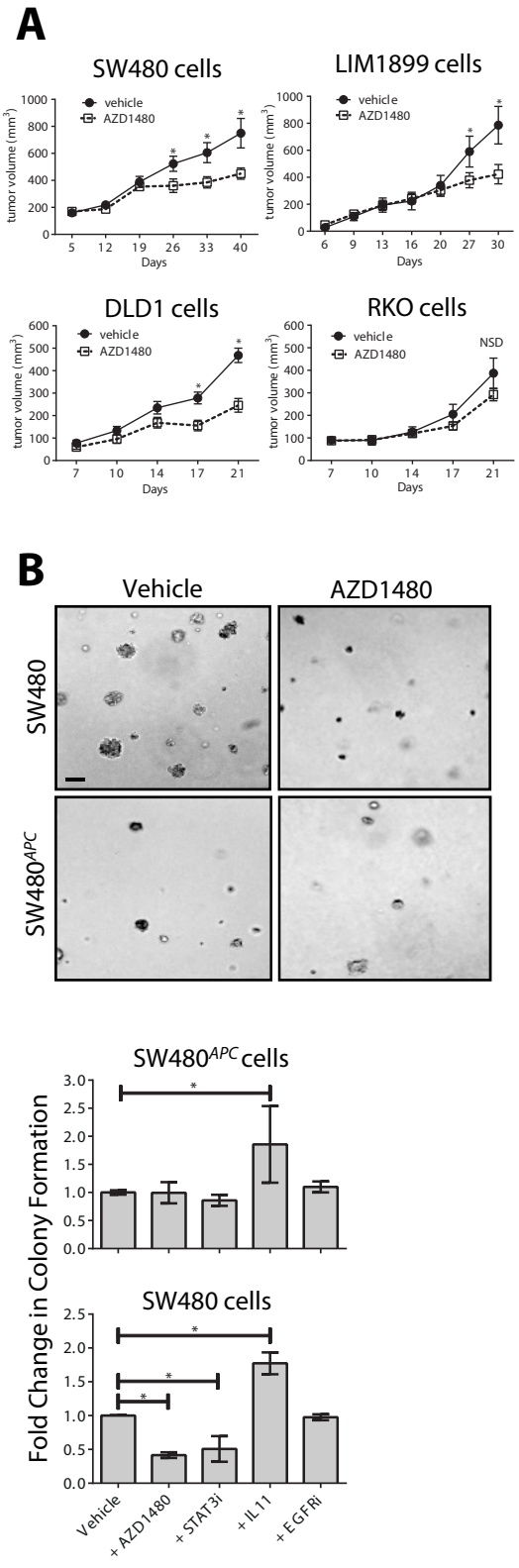
A
SW480 cells
LIM1899 cells
DLD1 cells
RKO cells
vehicle
AZD1480
tumor volume (mm3)
Days
NSD
B
Vehicle
AZD1480
SW480
SW480APC
SW480APC cells
SW480 cells
Fold Change in Colony Formation
Vehicle
+AZD1480
+STAT3i
+IL 11
+EGFRi

Figure 6

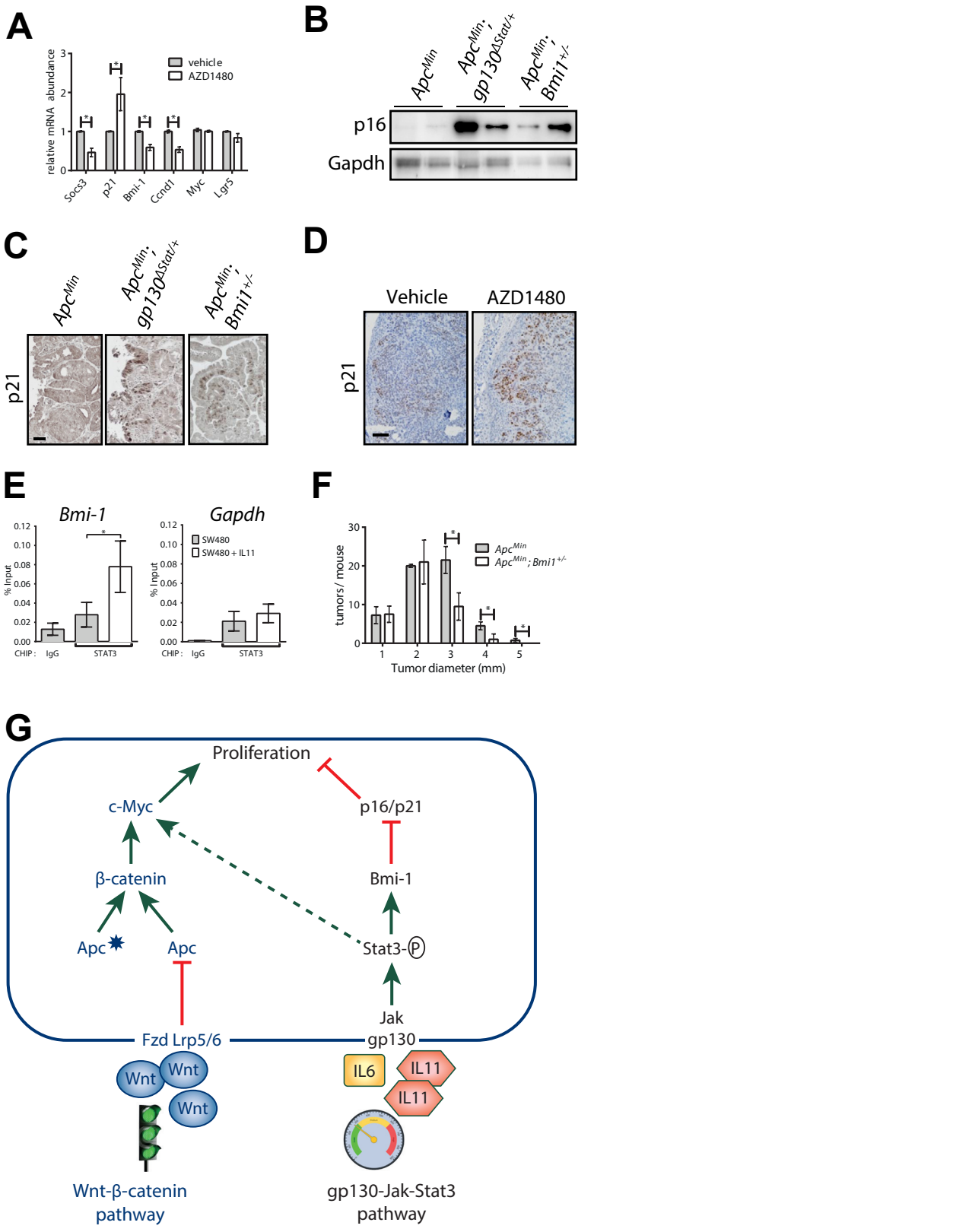
A
relative mRNA abundance
vehicle
AZD1480
Socs3
p21
Bmi-1
Ccnd1
Myc
Lgr5
B
Apc^Min
Apc^Min; gp130^ΔStat1/+
Apc^Min; Bmi1^+/-
p16
Gapdh
C
Apc^Min
Apc^Min; gp130^ΔStat1/+
Apc^Min; Bmi1^+/-
p21
D
Vehicle
AZD1480
p21
E
Bmi-1
Gapdh
% Input
SW480
SW480 + IL11
CHIP: IgG
STAT3
F
tumors / mouse
Apc^Min
Apc^Min; Bmi1^+/-
Tumor diameter (mm)
G
Proliferation
c-Myc
p16/p21
β-catenin
Bmi-1
Apc
Apc
Stat3-P
Jak
gp130
Fzd Lrp5/6
Wnt
Wnt
Wnt
IL6
IL11
IL11
Wnt-β-catenin pathway
gp130-Jak-Stat3 pathway

Supplementary Materials

Fig. S1	**gp130-Jak-Stat3 signaling regulates intestinal regeneration and tumorigenesis.**
Fig. S2	**gp130-Jak-Stat3 signaling limits induced colonic tumorigenesis in in *Lgr5*^{CreERT2}; *Apc*$^{fl/fl}$ mice and human CRC xenografts.**
Fig. S3	**Gene signature for Wnt and gp130-Jak-Stat3 signaling co-exist in human colorectal cancers.**
Fig S4	**Xenograft growth is supressed by partial inhibition of the gp130/Jak/Stat3 pathway without effecting Stat1.**
Fig. S5	**Stimulation of gp130-Jak-Stat3 signaling does not affect aberrant Wnt-β-catenin signalling in the SW480 human CRC cell line.**
Fig. S6	**Inhibition of gp130-Jak-Stat3 signaling does not affect intestinal homeostasis.**
Fig. S7	**Inhibition of gp130-Jak-Stat3 signaling relieves Bmi1-mediated repression of the gene encoding p21 intestinal tumors.**
Table S1	**Primer sequences used for RT-qPRC**

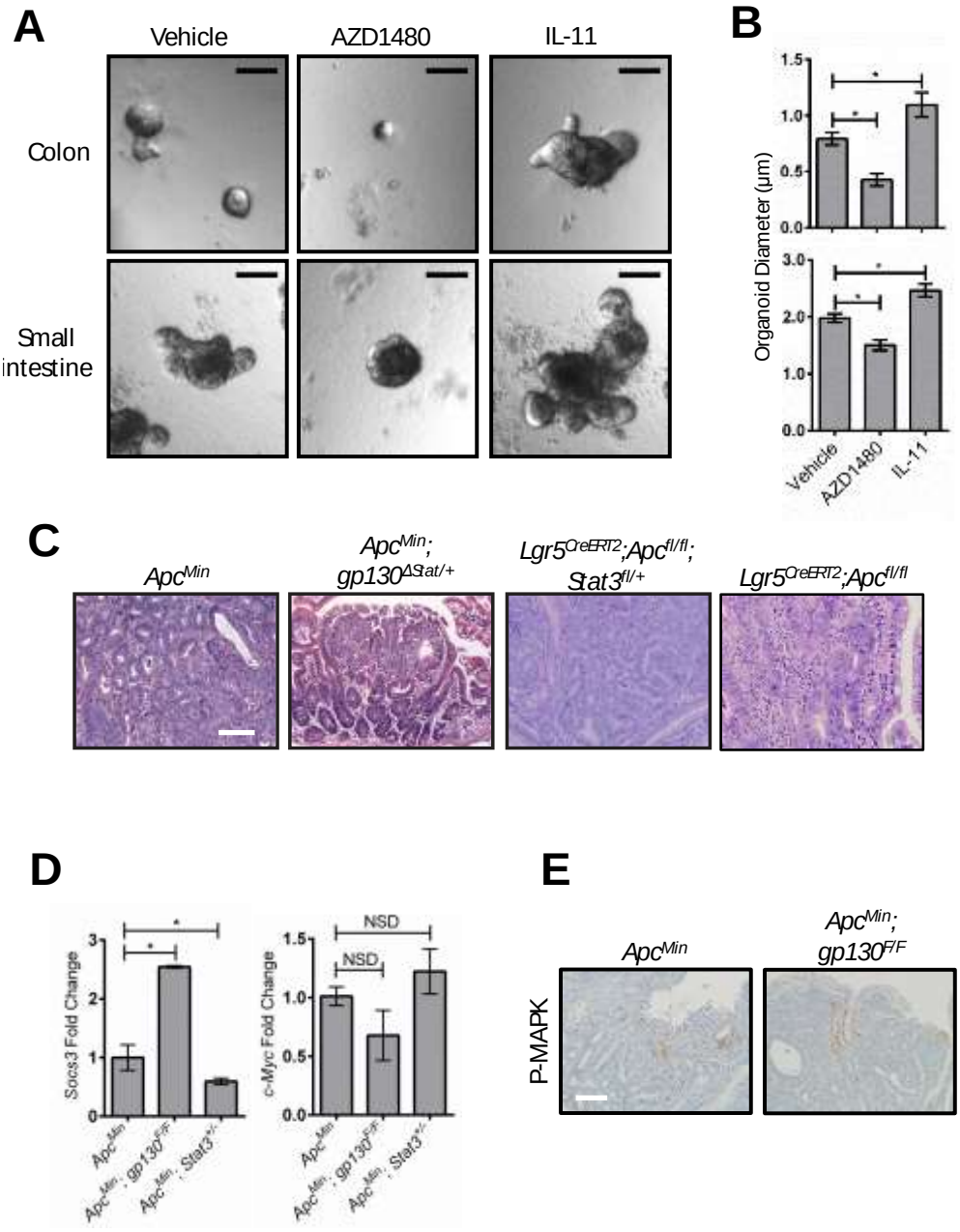

Figure S1. gp130-Jak-Stat3 signaling is required for intestinal regeneration and tumorigenesis.
(A) Photomicrographs of organoids grown from crypts from the colon or small intestine of wild-type mice exposed to vehicle (DMSO), AZD1480 (2µM) or IL-11 (10ng/ml) for 7 days. Scale bar = 100 µm. **(B)** Quantification of organoid size from cultures depicted in (A). Data are mean ± SEM of duplicate cultures from 2 independent experiments. * $p \leq 0.04$. Mann-Whitney U-test. **(C)** Photomicrographs of haematoxylin- and eosin-stained sections of intestinal tumors of 150 day old $Apc^{Min/+}$ and $Apc^{Min/+}$;$gp130^{F/F}$, or of $Lgr5Cre^{ERT2/+}$;$Apc^{fl/fl}$;$Stat3^{fl/+}$ 36d after tamoxifen are non-invasive and display characteristics of tubular adenomas. Scale bar = 100 µm. Images are representative of 3mice. **(D)** Relative abundance of the mRNA for the Stat3 target gene *Socs3* and for the Wnt-β-catenin target gene *c-Myc* in intestinal tumors of 100 day old mice of the indicated genotypes. Data are mean ± SEM of 3 mice per cohort. * $p \leq 0.04$. Mann Whitney U-test. NSD = not significantly different. **(E)** Immunohistochemical staining for phosphorylated MAPK (Erk1/2) Thr202/Tyr204 MAPK in intestinal tumours of mice of the indicated genotypes. Images are representative of 3 mice.

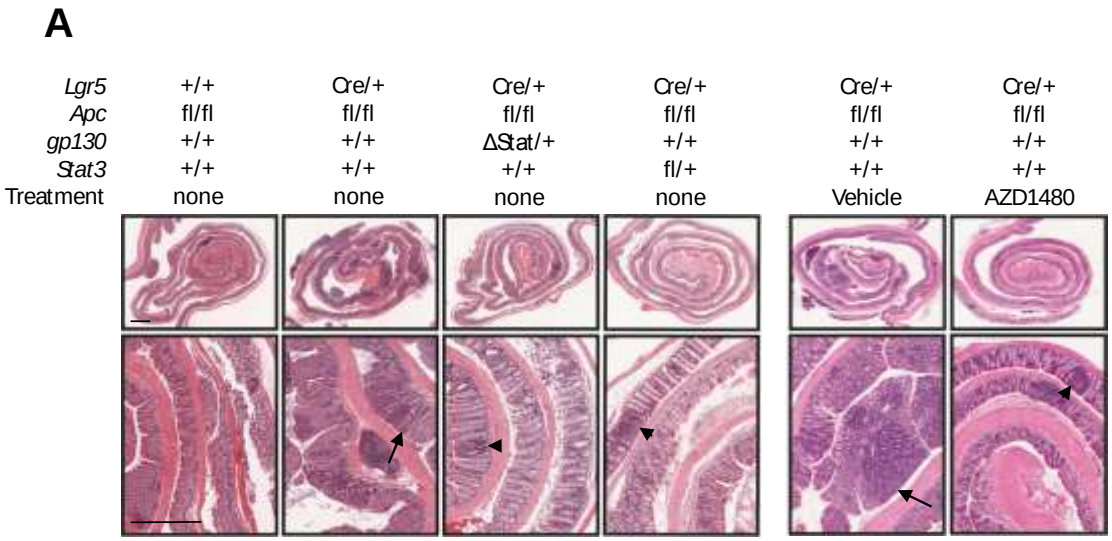

Figure S2. gp130-Jak-Stat3 signaling limits colon tumorigenesis in *Lgr5*^{CreERT2}; *Apc*$^{fl/fl}$ mice and human CRC xenografts. (A) Haematoxylin- and eosin-stained cross-sections of colons from mice of the indicated genotypes collected 35 days after tamoxifen administration. Some mice also received 35 days of daily gavage of AZD1480 (30mg/kg, daily) or vehicle. Neoplastic foci (arrowhead) and tubular adenomas (arrows) are indicated. Scale bar = 1mm.

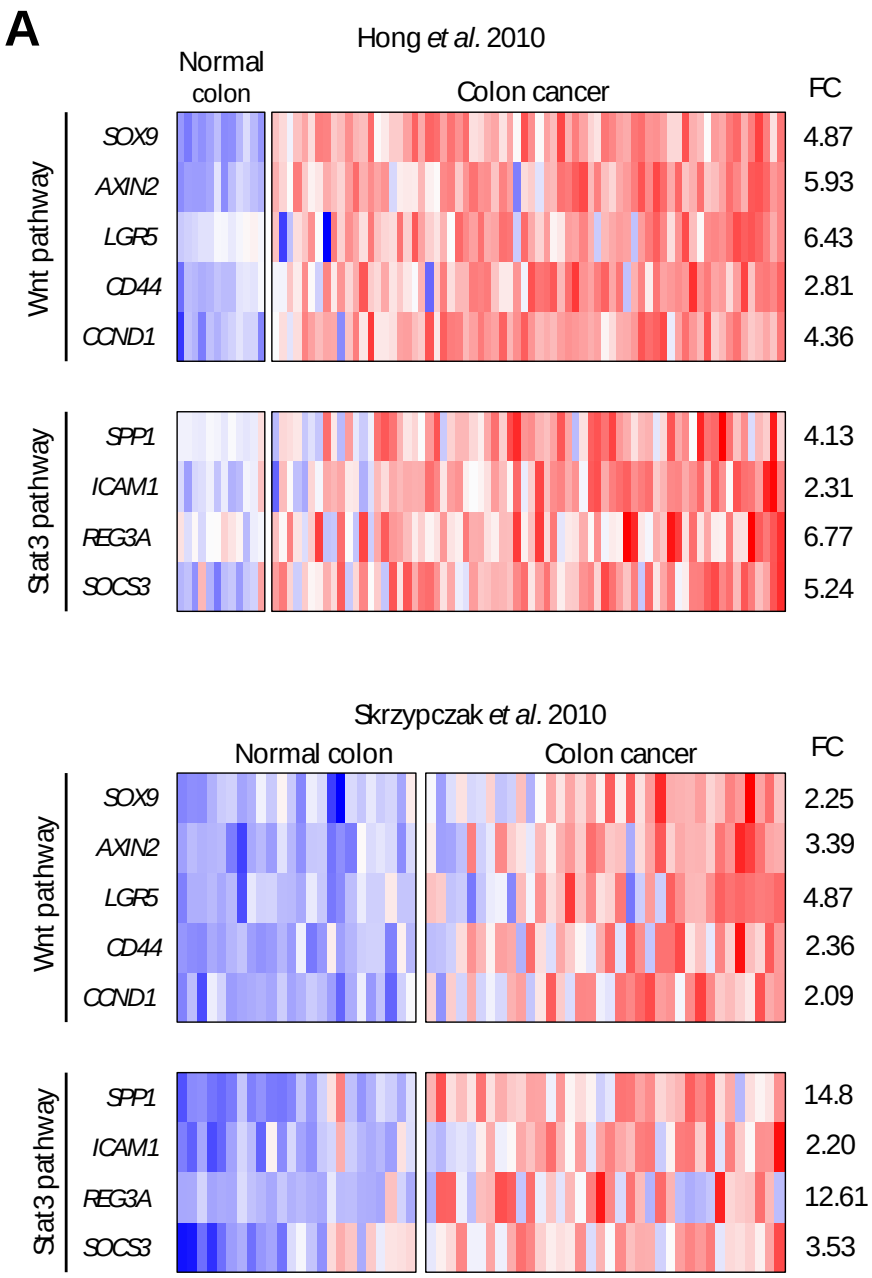

Fig. S3. Gene signature for Wnt and gp130-Jak-Stat3 signaling co-exist in human colorectal cancers.
Heatmaps of the Z-scores representing the relative abundance of mRNAs of β-catenin and Stat3 target genes in CRC and normal colon biopsies. Oncomine (http://oncomine.org) was used to extract data from 12 normal and 70 CRC samples from Hong *et al*. [GSE9348; (*27*)] and from 24 normal and 36 CRC samples from Skrzypczak *et al*. [GSE20916; (*28*)]. Z-scores were calculated by subtracting the mean for the corresponding gene probe and dividing by the standard deviation. Individual samples are aligned vertically and ordered according to the average Z-score across samples. Fold change (FC) was calculated as the mean of CRC samples divided by the mean of control samples for each gene. $p < 0.001$ comparing normal to CRC samples for each gene. Mann-Whitney U test.

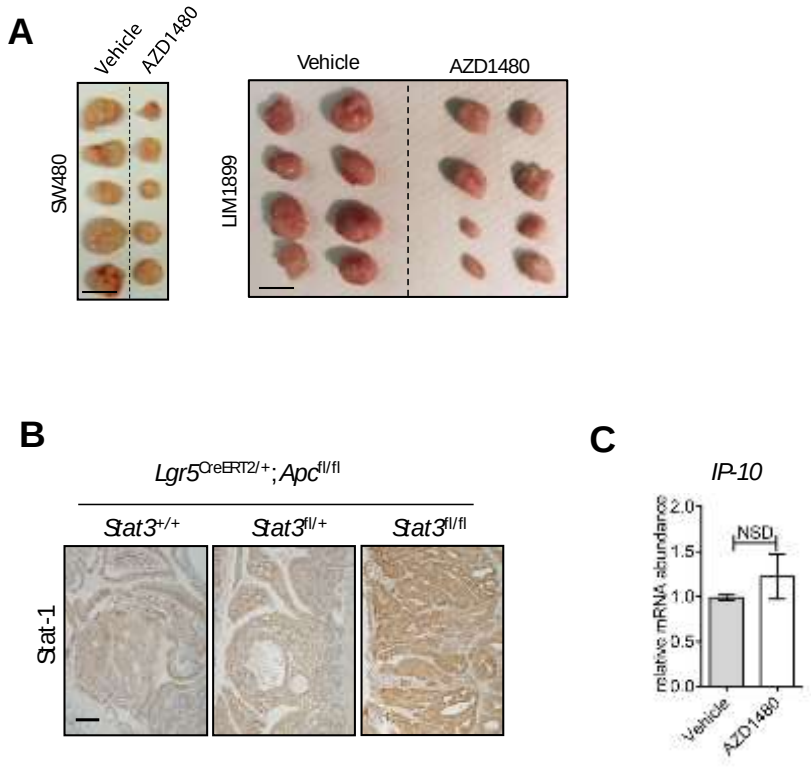

Fig S4. Xenograft growth is supressed by partial inhibition of the gp130-Jak-Stat3 pathway without effecting Stat1. (A) Tumor xenografts resected from BALB/c-nude mice injected subcutaneously with human SW480 or LIM1899 CRC cell lines and gavaged daily with AZD1480 (30 mg/kg) or vehicle starting on the 5th day after cell injection. Photograph of representative tumors were taken 40 (SW480 cells) or 30 (LIM1899 cells) days after cell injection. Scale bar = 1 cm **(B)** Immunohistochemical analysis for Stat1 in intestinal tumours from mice of the indicated genotype 36 days after tamoxifen administration. Images are representative of 3 mice. **(C)** Quantification of the relative mRNA abundance for the interferon-γ-Stat1 target gene *IP-10* in xenografts resected from AZD1480 and vehicle-treated mice from Fig. 5A (n = 3 mice).

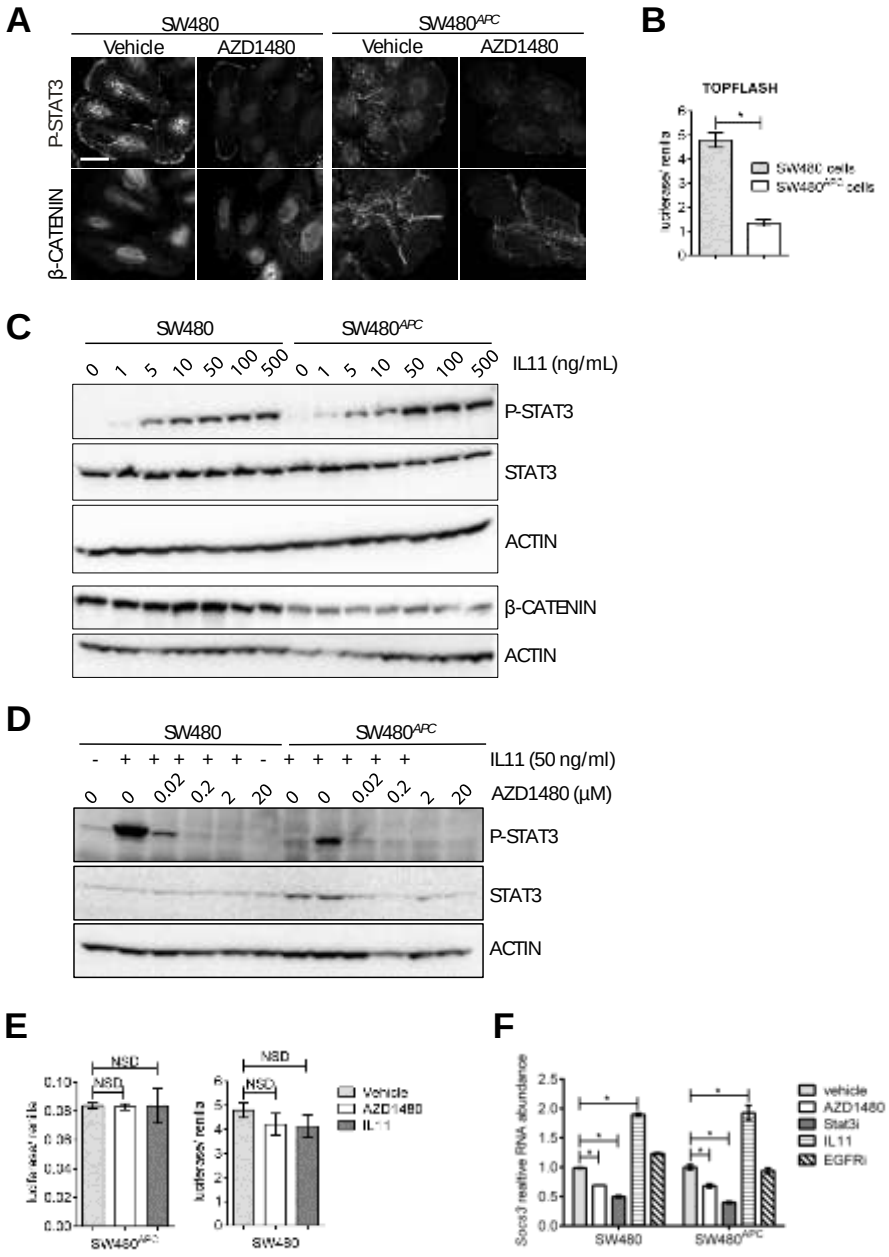

Figure S5. Stimulation of gp130-Jak-Stat3 signaling does not affect aberrant Wnt-β-catenin signalling in the SW480 human CRC cell line. (A) Immunofluorescence staining for β-catenin or phosphorylated Tyr^{205} Stat3 (P-Stat3) in SW480 and SW480^{APC} cells after exposure to vehicle (DMSO) or AZD1480 (2μM). Scale bar = 20 μm. **(B)** TOPFLASH-reporter activity in SW480 and SW480^{APC} cells. Luciferase activity was normalized to Renilla luciferase. Data are mean ± SEM of triplicates from 3 independent experiments. *p = 0.04; Mann-Whitney U-test. **(C and D)** Western blot analysis for phosphorylated Tyr^{205} Stat3 (P- Stat3), total Stat3 (Stat3) and β-catenin in SW480 or SW480^{APC} cells after 30 min exposure to the indicated amount of IL11 and AZD1480. Actin was used as a loading control. **(E)** TOPFLASH-reporter activity in SW480 and SW480^{APC} cells exposed to AZD1480 (2μM) or IL11 (50ng/ml) for 30 min. Data are mean ± SEM of triplicates from 3 independent experiments. NSD = not significantly different. Mann-Whitney U-test. **(F)** Quantification of the relative mRNA abundance of the Stat3 target gene *Socs3* in SW480 and SW480^{APC} cells grown for 10 days under colony forming conditions in soft agar in the presence of AZD1480 (2μM), Stat3 inhibitor S3I-201 (50μM), IL11 (10ng/ml), EGFR inhibitor AG1478 (1μM), or vehicle (DMSO). Data are normalized to the vehicle-treated SW480 cells arbitrarily set as 1 and represent the mean ± SEM of triplicates from 3 independent experiments. * $p \leq 0.04$. Mann-Whitney U-test.

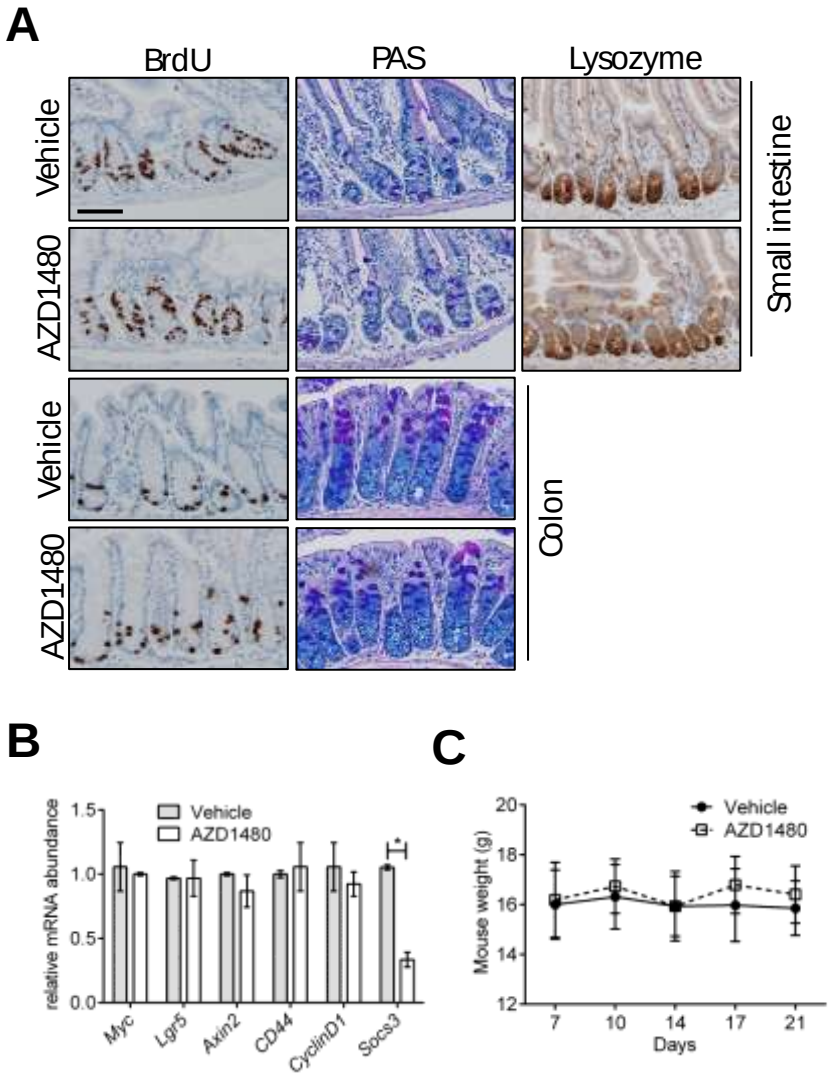

Figure S6. Inhibition of gp130-Jak-Stat3 signaling does not affect intestinal homeostasis.
(A) Immunohistochemical analysis of cell proliferation (BrdU), goblet cells (periodic acid-Schiff, PAS), and Paneth cells (lysozyme) in the small intestines of BALB/c-nude mice gavaged daily with AZD1480 (30mg/kg) or vehicle from day 5 to 21 after SW480 cell xenograft injection. Scale bar = 50 μm. Images are representative of 6 mice. **(B)** Quantification of the relative mRNA abundance for Wnt/β-catenin target genes, and *Socs3*, in IECs isolated from BALB/c-nude mice shown in Fig. 5A, or **(C)** body weight of the same mice. Data are mean ± SEM of at least 5 mice per cohort. * $p \leq 0.04$. Mann-Whitney U-test.

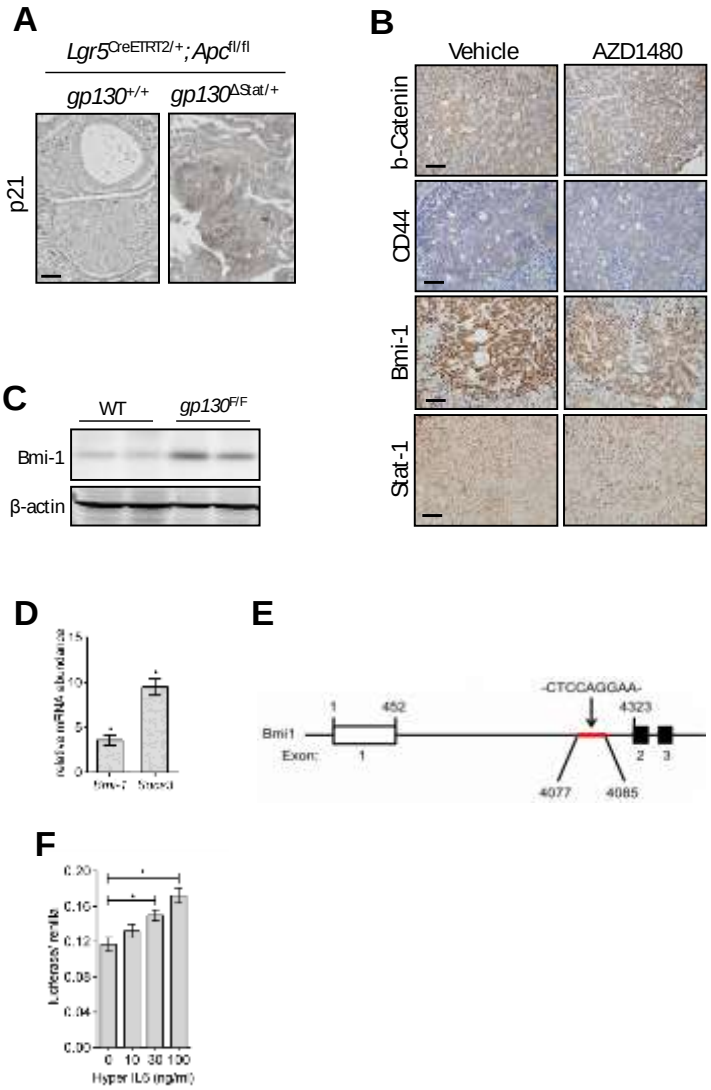

Figure S7. Inhibition of gp130-Jak-Stat3 signaling relieves Bmi1-mediated repression of the gene encoding p21 intestinal tumors. (A) Immunohistochemical analysis for p21 on intestinal tumors from with the indicated genotypes 36 days after tamoxifen administration. Images are representative of 6 mice. **(B)** Immunohistochemical analysis of sections of SW480 tumor xenografts from Balb/C nude mice gavaged daily for 40 days with AZD1480 or vehicle from Fig. 5A. Images are representative of 6 mice. **(C)** Western blot analysis for Bmi-1 in lysates of IECs isolated from wild-type (WT) and *gp130*$^{F/F}$ mice. β-actin was used as a loading control. Each lane represents an individual mouse. **(D)** Quantification of the relative mRNA abundance for *Socs3* and *Bmi-1* in IECs isolated from *gp130*$^{F/F}$ mice 30 minutes after a single intraperitoneal injection of recombinant IL11 (5µg). Fold changes was calculated by comparing mRNA from IEC isolated from unijected mice. Data are mean ± SEM of 3 mice per condition. * $p \leq 0.04$. Mann-Whitney U-test. **(E)** Schematic outline of the position of the putative Stat3 binding site (red line) in intron 1 of the murine *Bmi-1* gene. A 555 base pair fragment encompassing this sequence was amplified to construct the *pBmi1:luc* Luciferase reporter. The open box denotes non-coding exon 1, black boxes indicate coding exons 2 and 3. **(F)** Relative luciferase activity in HEK293T cells transfected with *pBmi1:luc* and *pCMV-Renilla* after 24h exposure to the indicated concentrations of Hyper IL6. *pBmi1:luc* activation was normalized to *Renilla* luciferase activity. Data are mean ± S.E.M. of triplicates from 3 independent experiments. * $p \leq 0.05$. Student's *t*-test.

CD44/for:	5’ - GTC TGC ATC GCG GTC AAT AG - 3’
CD44/rev:	5’ - GGT CTC TGA TGG TTC CTT GTT C - 3’
Cmyc/for:	5’ - TAG TGC TGC ATG AGG AGA CA - 3’
Cmyc/rev:	5’ - GGT TTG CCT CTT CTC CAC AG - 3’
CyclinD1/for:	5’ - GCA CAA CGC ACT TTC TTT CCA - 3’
CyclinD1/rev:	5’ - CGC AGG CTT GAC TCC AGA AG - 3’
Gapdh/for:	5' - CAA CTC ACT CAA GAT TGT CAG CAA - 3'
Gapdh/rev:	5' - TAC TTG GCA GGT TTC TCC AGG C - 3'
Socs3/for:	5' - GCG GGC ACC TTT CTT ATC C - 3'
Socs3/rev:	5' - TCC CCG ACT GGG TCT TGA C - 3'
Bmi1/forw:	5' - CAA AAC CAG ACC ACT CCT GAA - 3'
Bmi1/rev:	5' - TCT TCT TCT CTT CAT CTC ATT TTT GA - 3'
Axin2/forw:	5'- CCA TGA CGG ACA GTA GCG TA - 3'
Axin2/rev:	5' - GCC ATT GGC CTT CAC ACT - 3'
CyclinD2/forw:	5' - CAC CGA CAA CTC TGT GAA GC - 3'
CyclinD2/rev:	5' - TCC ACT TCA GCT TAC CCA ACA - 3'
Fzd7/forw:	5' - CGT CTT CAG CGT GCT CTA CA - 3'
Fzd7/rev:	5' - TCA TAA AAG TAG CAG GCC AAC A - 3'
Lgr5/forw:	5' - CTT CAC TCG GTG CAG TGC T - 3'
Lgr5/rev:	5' - GAT CAG CCA GCT ACC AAA TAG G - 3'
SOCS3/forw:	5' - GAC TTC GAT TCG GGA CCA G - 3'
SOCS3/rev:	5' - AAC TTG CTG TGG GTG ACC AT - 3'
CDKN1A/forw:	5' - TGC GTT CAC AGG TGT TTC TG - 3'
CDKN1A/rev:	5' - AGC TGC TCG CTG TCC ACT - 3'
BMI1/forw:	5' - CCA TTG AAT TCT TTG ACC AGA A - 3'
BMI1/rev:	5' - CTG CTG GGC ATC GTA AGT ATC - 3'
CCND1/forw:	5' - GCC GAG AAG CTG TGC ATC - 3'

CCDN1/rev:	5' - CCA CTT GAG CTT GTT CAC CA - 3'
CMYC/forw:	5' - GCT GCT TAG ACG CTG GAT TT - 3'
CMYC/rev:	5' - TAA CGT TGA GGG GCA TCG - 3'
LGR5/forw:	5' - ACC AGA CTA TGC CTT TGG AAA C - 3'
LGR5/rev:	5' - TTC CCA GGG AGT GGA TTC TAT - 3'
CXCL10/forw:	5' - GAA AGC AGT TAG CAA GGA AAG GT - 3'
CXCL10/rev:	5' - GAC ATA TAC TCC ATG TAG GGA AGT GA - 3'
GAPDH/forw:	5' - CCC CGG TTT CTA TAA ATT GAG C - 3'
GAPDH/rev:	5' - CAC CTT CCC CAT GGT GTC T - 3'

Table S1. Primer sequences used for RT-qPRC.